CHAPTER THIRTY-NINE

HYDROTHERMAL SYNTHESIS AND CRYSTAL STRUCTURES OF ACTINIDE COMPOUNDS

Thomas E. Albrecht-Schmitt, Peter C. Burns, and Sergey V. Krivovichev

39.1 Introduction 4157
39.2 Hydrothermal redox chemistry 4158
39.3 Structural chemistry of selected An(III) (An = Am, Cm, Cf) compounds 4162
39.4 Structural chemistry of selected An(IV) (An = Th, U, Np, Pu) compounds 4163
39.5 Structural chemistry of selected An(V) (An = U, Np, Pu) compounds 4170
39.6 Structural chemistry of An(VI) (An = U, Np, Pu) compounds 4178
39.7 Conclusions and perspectives 4186
References 4188

39.1 INTRODUCTION

Hydrothermal synthesis generally refers to the preparation of known and novel compounds in water at above-ambient conditions. A somewhat broader approach is taken here to include important compounds derived from ambient-temperature aqueous reactions. Hydrothermal preparative techniques are very old, and compounds such as barium carbonate were prepared in superheated water by Bunsen as early as the 1830s (Kolis and Korzenski, 1999). Since this time the methodology has undergone many revolutions and modifications centered around containing superheated water and the reactants therein at high temperatures and pressures. Much like actinide chemistry in general, hydrothermal synthesis was significantly advanced during World War II, when it became necessary to produce ultrapure α-quartz needed in microwave communication (Kolis and Korzenski, 1999). Continued searches for routes to electronic materials at Bell Laboratories and Philips Electronics lead to the fine-tuning of hydrothermal crystal growth conditions (Kolis and Korzenski, 1999). However, it was not until the discovery of the utility of hydrothermally-synthesized zeolites that work in this field expanded into many divergent areas. There is an important distinction that needs to be made in hydrothermal

chemistry between reactions that are occurring in superheated water and those that occur in supercritical water (>374°C). The vast majority of work in the field of hydrothermal synthesis of actinide compounds has taken place utilizing polytetrafluoroethylene (PTFE) lined autoclaves, placing the upper temperature limit at about 230°C. Far more specialized equipment is needed to perform reactions in supercritical water, and few actinide chemists have made this commitment (Bean *et al.*, 2001).

The application of hydrothermal synthetic methods to the preparation of a vast array of novel actinide compounds has occurred over the past decade. This chapter seeks to meet the goals of acquainting the reader with hydrothermal synthetic methods, the origins of the applications of these methods to preparation of crystalline actinide solids, and the structures of compounds derived from hydrothermal reactions. The beauty of this synthetic methodology is that it has been successfully applied to preparing Th, U, Np, Pu, Am, Cm, and Cf compounds in oxidation states ranging from +3 to +6. These reactions have ranged in scale from grams to micrograms and yet have all resulted in the growth of crystals of sufficient quality for X-ray diffraction studies and physical property measurements.

39.2 HYDROTHERMAL REDOX CHEMISTRY

One of the challenges that hydrothermal reaction conditions present is that they are far from the experimental conditions used to derive predictive thermodynamic and kinetic values. A variety of reduction reactions have been uncovered from hydrothermal conditions that have yet to be observed at ambient temperature and pressure. There has been some conjecture that hydrothermal conditions merely act to artificially age systems where the reaction kinetics are slow. However, the situation is likely to be more complex than this. The neptunium iodate system aptly illustrates the complexity of hydrothermal redox reactions (Bray *et al.*, 2007a).

The reaction of NpO_2 with iodate under acidic conditions results in the formation of five distinct products with Np oxidation states ranging from +4 to +6, depending on the experimental conditions.

$$5NpO_2 + 12H^+ + 2IO_3^- \xrightarrow[H_2O]{200^\circ C,\ 3\ d} 5NpO_2^{2+} + I_2 + 6H_2O \tag{39.1}$$

$$2NpO_2^{2+} + 4H^+ \xrightarrow[<375\ \mu L\ H_2O]{200^\circ C,\ 3\ d} 2Np^{4+} + 2H_2O + O_2 \tag{39.2}$$

$$Np^{4+} + 4IO_3^- \xrightarrow[100\ \mu L\ H_2O]{200^\circ C,\ 3\ d} Np(IO_3)_4 \tag{39.3}$$

$$2Np^{4+} + 8IO_3^- + nH_2O \xrightarrow[250\ \mu L\ H_2O]{200^\circ C,\ 3\ d} Np(IO_3)_4 + Np(IO_3)_4 \cdot nH_2O \quad (39.4)$$

$$NpO_2^{2+} + Np^{4+} + 2IO_3^- + 2H_2O \xrightarrow[375\ \mu L\ H_2O]{200^\circ C,\ 3\ d} 2NpO_2(IO_3) + 4H^+ \quad (39.5)$$

$$2NpO_2^{2+} + 4IO_3^- + 2H_2O \xrightarrow[500\ \mu L\ H_2O]{200^\circ C,\ 3\ d} NpO_2(IO_3)_2 \cdot H_2O + NpO_2(IO_3)_2(H_2O) \quad (39.6)$$

Reaction 39.1 describes the direct two-electron oxidation of Np^{4+} to NpO_2^{2+} by iodate. Acidic dissolution of NpO_2 in the presence of oxygen typically yields Np(V) in the form of NpO_2^+ in solution. Reaction 39.1 is governed by the strong oxidizing potential of iodate under acidic conditions that is sufficient to directly oxidize Np^{4+} to NpO_2^{2+}. The standard potentials for these reactions are given below (Morss *et al.*, 2006; Bard *et al.*, 1985).

$$NpO_2^{2+} \xrightarrow{1.16\ V} NpO_2^+ \xrightarrow{0.60\ V} Np^{4+} \quad (0.88\ V)$$

$$2IO_3^- + 12H^+ + 10e^- \xrightarrow{1.20\ V} I_2 + 6H_2O$$

It is important to note that these E° values are given at 25°C and 1 atm. Reactions 39.1 through 39.7 are occurring at 200°C and approximately 17 atm (if H_2O exhibits the vapor pressure of pure water), and therefore these standard potentials can only be used for guidance. However, the reduction potentials for NpO_2^{2+} are known up to 300°C, and they are essentially invariant with increasing temperature. In contrast, the oxidation potential of water changes from approximately 1.23 V at 25°C to 1.02 V at 300°C. Therefore, water is more easily oxidized at higher temperatures. When the reactions occur with only a limited amount of liquid water present, as is demonstrated in reactions 39.2 and 39.7, reduction of NpO_2^{2+} back to Np^{4+} takes place. These reactions might be termed precipitation-driven redox reactions; where the formation of a highly insoluble product is one of the primary driving forces for the reaction to take place. Further evidence for this type of reaction comes from reaction 39.7, where $Np(IO_3)_4$ (and its hydrate) form via the oxidation of water and reduction of Np(VI) despite the fact that there is a large excess of an oxidizing agent present.

$$2H^+ + NpO_2(IO_3)_2 \cdot H_2O + 2IO_3^- \xrightarrow[250\ \mu L\ H_2O]{200^\circ C,\ 3\ d} Np(IO_3)_4 + 2H_2O + 1/2O_2 \quad (39.7)$$

When sufficient amounts of water are present to approximate a solution (500 μL), as in reaction 39.6, the predicted reaction between NpO_2 and iodate

occurs, via reaction 39.1, and $NpO_2(IO_3)_2(H_2O)$ and $NpO_2(IO_3)_2 \cdot H_2O$ form (Bean *et al.*, 2003). Reaction 39.5 is the most interesting of this series, and represents conditions under which comproportionation of Np^{4+} and NpO_2^{2+} occurs to yield two equivalents of NpO_2^+. In terms of concentrations at room temperature, the reaction with 333 μL of water would be 0.037 M in neptunium. In a typical reaction there is a tenfold excess of iodic acid.

The sequence of reactions 39.2 through 39.4 is not solely driven by the solution phase thermodynamics of the oxidation of Np^{4+} by iodate, but also by the reduction of Np(VI) to yield Np(IV), and the subsequent crystallization of the Np(IV) iodate products, $Np(IO_3)_4$ and $Np(IO_3)_4{\cdot}nH_2O{\cdot}nHIO_3$. It has been noted that when solutions of NpO_2^+ are hydrothermally treated at 200°C that crystalline NpO_2 forms (Roberts *et al.*, 2003). These results might suggest that aqueous Np(V) might not dominate the chemistry of neptunium under geological conditions, such as those found in an underground repository, nearly as much as previously thought.

As was observed with neptunium, the reaction of PuO_2 with iodate leads to the two-electron oxidation of Pu^{4+} to PuO_2^{2+} with concomitant production of elemental iodine (reaction 39.8).

$$5PuO_2 + 12H^+ + 2IO_3^- \xrightarrow[H_2O]{200^\circ C,\ 3\ d} 5PuO_2^{2+} + I_2 + 6H_2O \tag{39.8}$$

$$Pu^{4+} + 4IO_3^- \xrightarrow[100\text{-}1,000\ \mu L\ H_2O]{200^\circ C,\ 3\ d} Pu(IO_3)_4 \tag{39.9}$$

In contrast to the NpO_2 reactions, the reaction of PuO_2 with iodate with up to 1,000 μL of water leads to the formation of $Pu(IO_3)_4$ (reaction 39.9). These results imply that the hydrothermal chemistry of plutonium iodates is dominated to an even greater extent than in the neptunium reactions by the solubility-driven formation of the An(IV) iodates.

In previous work it was shown that stock solutions of Pu^{4+} and NpO_2^+ react with excess metaperiodate, IO_4^-, to yield products that contain the actinides in the +6 oxidation state (e.g. $NpO_2(IO_3)_2(H_2O)$ and $AnO_2(IO_3)_2 \cdot H_2O$ (An = Np, Pu)) (Bean *et al.*, 2003; Runde *et al.*, 2003). Metaperiodate contains I(VII), and is a much stronger oxidant than iodate (1.60 vs 1.20 V) (Bard *et al.*, 1985). Clearly, the reactions reported herein of AnO_2 (An = Np, Pu) with iodate under hydrothermal conditions with limited amounts of water are dramatically different from those of aqueous actinide ions with very strong oxidants. While these reactions are occurring at a much lower pH than natural groundwaters, this work calls into question the use of standard solution reactivity data on actinide ions to predict the behavior of spent nuclear fuels (SNF) that will start off as a reduced solid. The thermodynamic data for actinide complexation are already being reevaluated in light of the substantial changes that occur at elevated temperatures (Rao *et al.*, 2004).

Hydrothermal reduction reactions can be used to rationally prepare actinide compounds in specified oxidations states. Very recently the in situ hydrothermal reduction of Np(VI) to Np(IV) has been used to prepare Np(IV) phosphonates. There are several curious features about the reaction of Np(VI) stock solutions with phosphonates that starts with the dramatic color change from pink to green that occurs upon addition of the phosphonate. UV-vis-NIR spectroscopic studies indicate that this color change corresponds to complexation of the NpO_2^{2+} cation by the phosphonate ligand (the use of phosphonoacetate allows everything to remain in solution), and that no redox chemistry occurs. The subjection of Np(VI) stock solution to hydrothermal treatment leads to the oxidization of water, and a mixture of Np(VI) and Np (V) is obtained (reaction 39.10). The subsequent reduction of Np(V) to Np(IV) might occur via two different pathways. In reaction 39.11 a precipitation-driven redox reaction is suggested. In reaction 39.12, the Np(IV) arises from disproportionation of Np(V) at low pH. The formation of a highly insoluble Np(IV) phosphonate would drive these reactions to completion in both cases (Nelson *et al.*, 2008a).

$$4NpO_2^{2+} + 2H_2O \xrightarrow[H_2O]{180^\circ C,\ 3\ d} 4NpO_2^{+} + 4H^{+} + O_2 \tag{39.10}$$

$$4NpO_2^{+} + 8CH_3PO_3H_2 \xrightarrow{180^\circ C,\ 3\ d} 4Np(CH_3PO_3)_2(s) + 6H_2O + O_2 + 4H^{+} \tag{39.11}$$

$$2NpO_2^{+} + 2CH_3PO_3H_2 \xrightarrow{180^\circ C,\ 3\ d} Np(CH_3PO_3)_2(s) + NpO_2^{2+} + 2H_2O \tag{39.12}$$

One of the most dramatic examples of hydrothermal reduction of an actinide comes from the preparation and characterization of $K_3(U_3O_6)(Si_2O_7)$ and $Rb_3(U_3O_6)(Ge_2O_7)$, both of which contain uranium in the rare +5 oxidation state (Lin *et al.*, 2008). These compounds were prepared using UO_3 as a starting material and the reactions were carried-out at 600°C (i.e. an atypical example of the use of supercritical water). Additional examples of hydrothermal reduction chemistry involving an actinide come from the uranyl chromates $A[(UO_2)_2Cr_2O_8](H_2O)_n$ (A = K_2, Rb_2, Cs_2, Mg; n = 0 or 4). In this case it is not the actinide that is reduced, but rather, as supported by bond-valence analyses, Cr(VI) is reduced to the rare oxidation state of Cr(V) that is trapped in the form of uranyl chromate sheet (Locock *et al.*, 2004). Finally, it has been noted in many publications that U(VI) can be reduced to U(IV) in the presence of organic molecules, in particular organoamines (Almond *et al.*, 2000). This has been observed in fluorides, oxyfluorides, and phosphates. In these reactions, the amines are likely serving as the reducing agents, not the water.

39.3 STRUCTURAL CHEMISTRY OF SELECTED An(III) (An = Am, Cm, Cf) COMPOUNDS

The structural chemistry of actinide compounds has been reviewed in part in previous volumes of this work. Here we present selected compounds derived from hydrothermal reactions that have not been previously discussed. An(III) (An = Am, Cm, Cf) compounds are represented by a small group primarily because isotopes of these elements pose special handling considerations that are not nearly as much of an issue with ^{237}Np and ^{239,242}Pu. Hydrothermally prepared compounds with these elements are only known with iodate, and all of them can be formulated as $An(IO_3)_3$. For $Am(IO_3)_3$ two different forms are known and have been represented as both type I (α-) iodates that are isostructural with $Gd(IO_3)_3$ (Sykora *et al.*, 2004), and type II β-$Am(IO_3)_3$ which is isostructural with $Bi(IO_3)_3$ (Runde *et al.*, 2006). $Cm(IO_3)_3$ adopts the type I structure shown in Fig. 39.1. $Cf(IO_3)_3$ is found to adopt the $Bi(IO_3)_3$ structure type (Sykora *et al.*, 2006).

Undoubtedly there are small energetic differences between these structures, and the crystallization of these compounds is highly sensitive to the hydrothermal conditions, pH, and stoichiometry. In each case these compounds were prepared via an interesting hydrothermal redox reaction whereby metaperiodate, IO_4^-, is reduced to IO_3^-. This technique was developed because $An(IO_3)_3$ compounds are quite insoluble in water and the direct addition of An^{3+} to IO_3^- results in the formation of powders. Metaperiodate compounds are much more soluble and dissolve under hydrothermal conditions, and are slowly

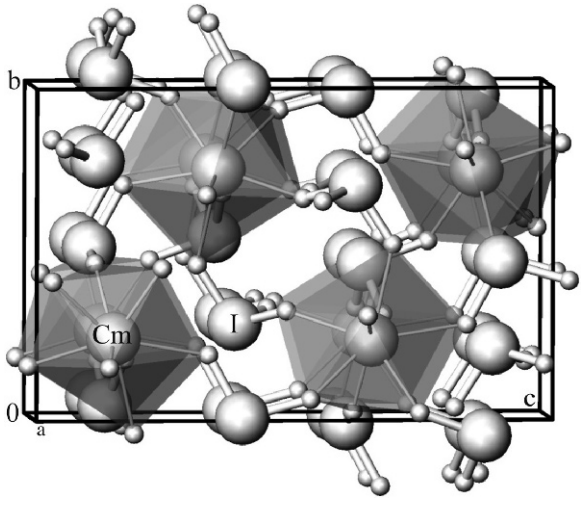

Fig. 39.1 *A view of the structure of the type* 1, *Cm*$(IO_3)_3$ (*adapted from Sykora et al.*, 2004). *Reproduced with permission from Elsevier*.

transformed via the oxidation of water into iodates. This process is apparently slow and results in the formation of high-quality single crystals.

39.4 STRUCTURAL CHEMISTRY OF SELECTED An(IV) (An = Th, U, Np, Pu) COMPOUNDS

An(IV) compounds prepared using hydrothermal techniques are far more numerous than An(III) compounds, being known with Th, U, Np, and Pu. The thorium compounds represent the smallest radiation hazard, and are the best developed. Although there are also many examples of U(IV) fluorides, only one will be discussed here.

The thorium compounds are known with iodate, fluoride, chromate, phosphate, sulfate, selenate, and mixed oxoanions similar to mineral phases have also been prepared (e.g. $Th(SeO_3)(SeO_4)$, $Th(IO_3)_2(SeO_4)(H_2O)_3{\cdot}H_2O$, and $Th(CrO_4)(IO_3)_2$). One common theme that differentiates An^{4+} compounds from AnO_2^{2+} compounds is the prevalence of three-dimensional networks. This is because the coordination geometry around the tetravalent actinides lends itself to three-dimensional connectivity, whereas with actinyl units the "yl" oxo atoms are typically terminal, so one direction of building is lost. Nevertheless, there are surprises in this chemistry that occur with the thorium iodates. There are at least three modifications of the $Th(IO_3)_4(H_2O)_n$ structure. Views of the structures of β-$Th(IO_3)_4(H_2O)$ and $Th(IO_3)_2(SeO_4)(H_2O)_3{\cdot}H_2O$ are shown in Figs. 39.2 and 39.3, respectively (Sullens *et al.*, 2006a, b). Both of these compounds are layered.

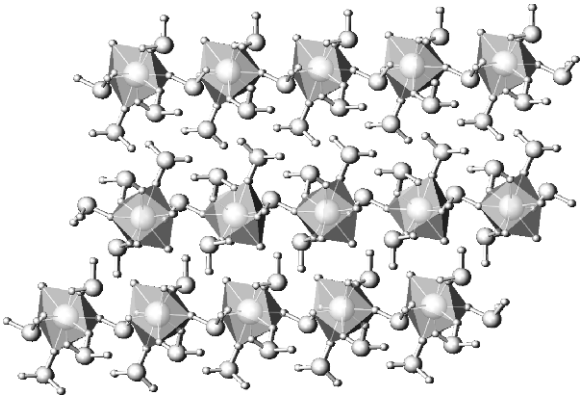

Fig. 39.2 *The view of β-$Th(IO_3)_4(H_2O)$ down the b-axis showing the two types of interdigitation of terminal iodate ligands that exist between the individual layers* (*adapted from Sullens et al.*, 2006a). *Reproduced with permission from the Materials Research Society.*

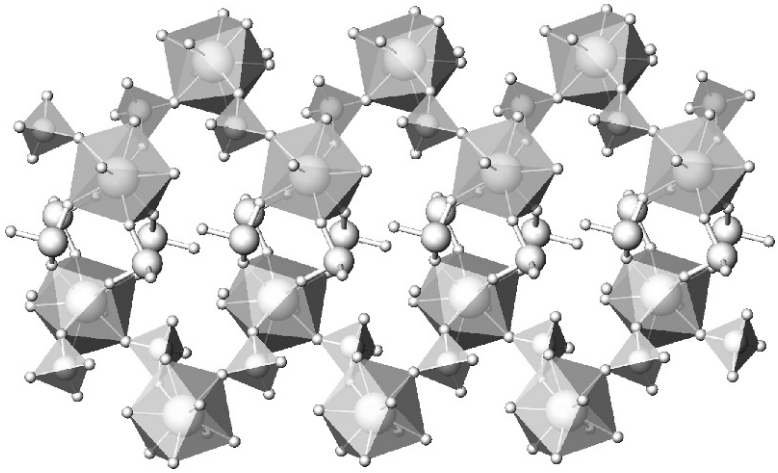

Fig. 39.3 *A view of part of a layer in* $Th(IO_3)_2(SeO_4)(H_2O)_3{\cdot}H_2O$ (*adapted from Sullens et al.*, 2006b). *Reproduced with permission from Elsevier*.

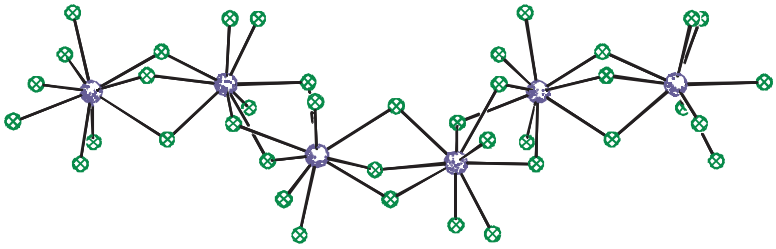

Fig. 39.4 *A view of the one-dimensional U(IV) fluoride chains in* $(C_5H_{14}N_2)_2U_2F_{12}{\cdot}2H_2O$. *This compound contains face-sharing tricapped trigonal prisms.*

Uranium(IV) fluorides are quite numerous and generally result from the reaction of uranium(VI) starting materials with HF in the presence of organic amines. For example, $(C_5H_{14}N_2)_2U_2F_{12}{\cdot}2H_2O$ was prepared from the reaction of UO_3 with HF and homopiperazine ($C_5H_{12}N_2$) at 200°C in aqueous media. A view of the structure of this compound is shown in Fig. 39.4 (Almond *et al.*, 2000).

Among the most interesting An(IV) compounds produced to date is actually a mixed-valent An(IV)/An(V) compound of neptunium. A view of the structure of the mixed-valent Np(IV)/Np(V) selenite, $Np(NpO_2)_2(SeO_3)_3$ is shown in Fig. 39.5 (Almond *et al.*, 2004). This compound results from the hydrothermal reaction of NpO_2 with SeO_2, and forms in the presence of numerous other cations.

The microscale precipitation of $Pu(IO_3)_4$ was used by B. B. Cunningham and L. B. Werner in 1942 to show, for the first time, that plutonium has a stable

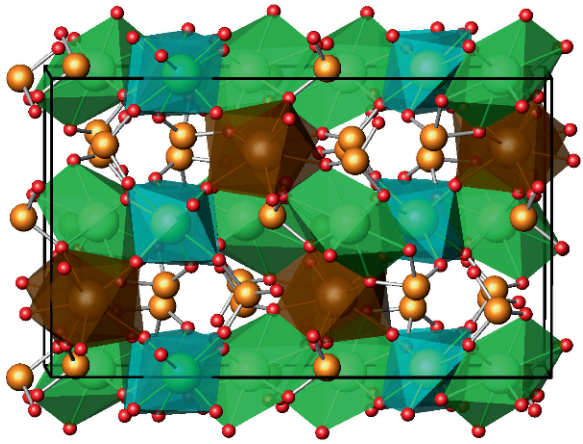

Fig. 39.5 *A view of the structure of the mixed-valent Np(IV)/Np(V) selenite, $Np(NpO_2)_2(SeO_3)_3$ (adapted from Almond et al., 2004). Reproduced with permission from the American Chemical Society.*

+4 oxidation state (Cunningham and Werner, 1949). Since this time $Pu(IO_3)_4$ has been used as a benchmark compound because of its remarkable insolubility in low pH media. The structure, precise elemental analyses, and spectroscopic data for Pu(IV) iodates had not been reported in the primary literature until 2007 (Bray *et al.*, 2007a). The structure is actually quite remarkable and consists of one-dimensional chains of trigonal dodecahedral Pu(IV) that are bridged by iodate. As noted above in the hydrothermal redox chemistry, $Np(IO_3)_4$ can also be synthesized via the hydrothermal reduction of Np(VI) in the presence of iodate. This compound is isostructural with its Pu(IV) analog (Bray *et al.*, 2007a). However, this structure type was first recognized in the literature from anhydrous Ce(IV) iodate, $Ce(IO_3)_4$ (Cromer and Larson, 1956; Staritsky and Cromer, 1956). The crystals of $Np(IO_3)_4$ and $Pu(IO_3)_4$ are both pleochroic and display a variety of different colors depending on the orientation of the crystal faces. This property is absent in $Ce(IO_3)_4$ (Fig. 39.6).

The first planned application of the in situ hydrothermal reduction of Np(VI) to Np(IV) was the preparation of the first transuranium phosphonate, $Np(CH_3PO_3)(CH_3PO_3H)(NO_3)(H_2O)\cdot H_2O$ (Bray, *et al.*, 2007b). This compound does not have an early transition metal, lanthanide, or uranium analog. Here we see a clear distinction between neptunium and other elements with potentially similar chemistry. The structure of this compound is shown in Fig. 39.7. This in situ method is a general one, and a variety of Np(IV) phosphonates have been prepared by this methodology.

A new class of heterobimetallic mixed-actinide compounds has recently been developed that contain two different actinides in two different oxidation states. The hydrothermal reaction of Np(VI) nitrate with UO_3 and methylenediphosphonic acid results in the formation of clusters of acicular pale green crystals

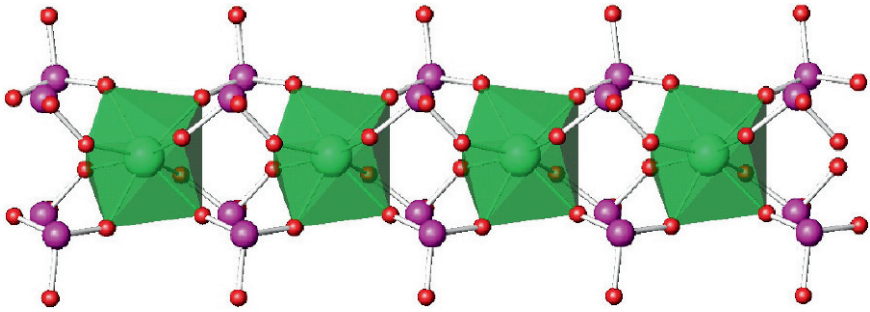

Fig. 39.6 *A view of the structure of* $An(IO_3)_4$ (*An = Ce, Np, Pu*) (*adapted from Bray et al.*, 2007a). *Reproduced with permission from the American Chemical Society.*

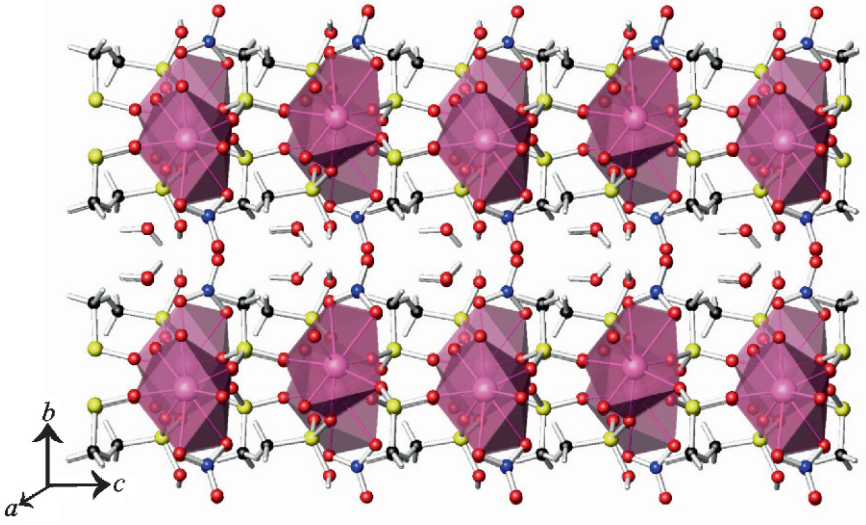

Fig. 39.7 *A view of the polar, lamellar structure of* $Np(CH_3PO_3)(CH_3PO_3H)(NO_3)(H_2O)\cdot H_2O$ (*adapted from Bray et al.*, 2007b). *Reproduced with permission from the American Chemical Society.*

of $UO_2Np(H_2O)_2[CH_2(PO_3)(PO_3H)]_2$ (Nelson, *et al.*, 2008b). The formation of this compound relies on the ability of methylenediphosphonate to simultaneously bind U and Np, as well as on the reduction of Np^{VI} to Np^{IV} under hydrothermal conditions, whereas the U^{VI} maintains its oxidation state in this reaction. The single crystal X-ray structure of $UO_2Np(H_2O)_2[CH_2(PO_3)(PO_3H)]_2$ reveals a remarkable three-dimensional framework structure constructed from UO_6 tetragonal bipyramids, NpO_8 distorted dodecahedra, and monoprotonated methylenediphosphonate anions, a view of which is shown in Fig. 39.8.

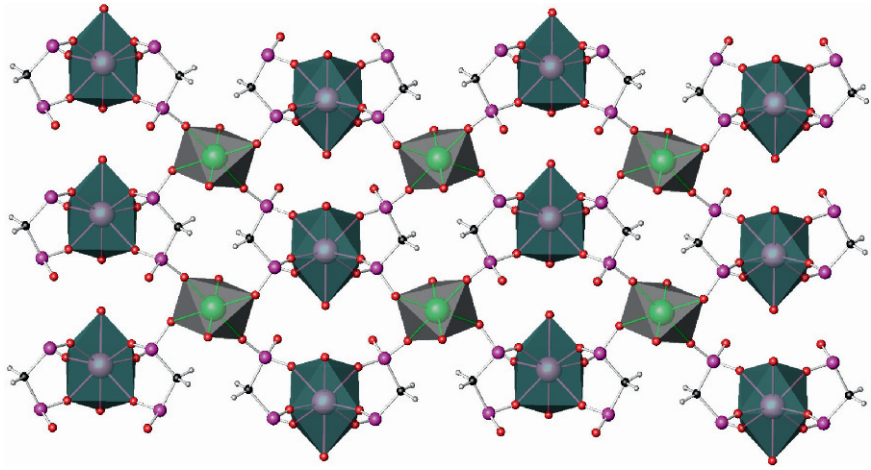

Fig. 39.8 *A view down the a-axis (in the [bc] plane) of the three-dimensional framework structure of the heterobimetallic U^{VI}/An^{IV} diphosphonate $UO_2An(H_2O)_2[CH_2(PO_3)(PO_3H)]_2$ (An = Th, Np, Pu) (adapted from Nelson et al., 2008b). Reproduced with permission from Wiley-VCH Verlag GmbH & Co.*

Attempts were made to prepare the mixed U(VI)/Pu(IV) using the same methods described above, but these reactions failed to produce heterobimetallic compounds. Instead the less clever reaction of UO_3 with PuO_2 and methylenediphosphonic acid results in the formation of the desired product $UO_2Pu(H_2O)_2[CH_2(PO_3)(PO_3H)]_2$, which is isotypic with its neptunium analog. The thorium analog of this compound can be prepared by this method as well (Nelson, *et al.*, 2009).

The reaction of NpO_2 with Cs_2CO_3, Ga_2O_3, H_3PO_4, and HF under mild hydrothermal conditions leads to the formation of $NpFPO_4$ after 4 days. Heating for an additional 6 days leads to the crystallization of $Cs_2Np_2F_7PO_4$ and NpF_4. The Ga_2O_3 forms a $GaPO_4$ matrix in which crystals of $NpFPO_4$, $Cs_2Np_2F_7PO_4$, and NpF_4 grow (Bray, *et al.*, 2007c). These fluorophosphates are also examples of Np(IV) compounds with three-dimensional structures. In the case of $NpFPO_4$ the structure is quite compact as shown in Fig. 39.9.

In contrast the structure of $Cs_2Np_2F_7PO_4$ is much more open and looks like a lamellar structure where the layers are joined in neptunium polyhedra as shown in Fig. 39.10.

Another example of an An(IV) compound comes from the simple of reaction of PuO_2 with SeO_2 under mild hydrothermal conditions. This reaction results in the formation of $Pu(SeO_3)_2$ (Bray *et al.*, 2008). This compound adopts the $Ce(SeO_3)_2$ structure type (Delage *et al.*, 1986), and consists of one-dimensional chains of edge-sharing $[PuO_8]$ distorted bicapped trigonal prisms linked by $[SeO_3]$ units into a three-dimensional network. An illustration of this structure is given in Fig. 39.11.

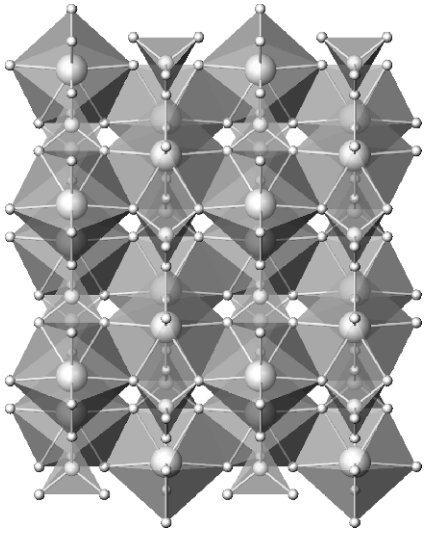

Fig. 39.9 *A view of the three-dimensional network of* $NpFPO_4$ (*adapted from Bray et al.*, 2007c). *Reproduced with permission from Elsevier*.

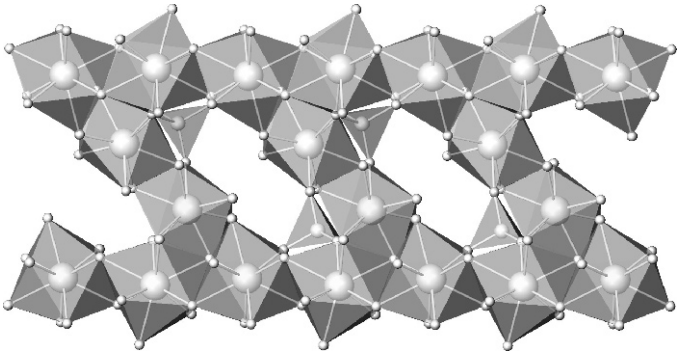

Fig. 39.10 *A view of the three-dimensional structure of* $Cs_2Np_2F_7PO_4$ (*adapted from Bray et al.*, 2007c). *Reproduced with permission from Elsevier*.

Another interesting U(IV) compound that resulted from U(VI) reduction is γ-UMo_2O_8 that forms as a result of hydrothermal reaction of uranyl acetate, Mo(VI) oxide and glycerin at 220°C (Krivovichev and Burns, 2004). This new modification of uranium(IV) molybdate is different from the two other modifications, α and β, prepared as a result of high-temperature solid-state reactions. In the structure of γ-UMo_2O_8, uranium atoms are in square antiprisms, whereas Mo(VI) atoms form MoO_4 tetrahedra (Fig. 39.12). The cation

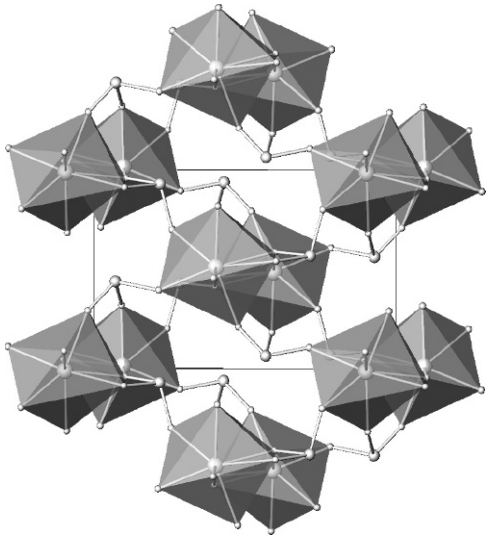

Fig. 39.11 *A view of the structure of* $Pu(SeO_3)_2$ (*adapted Bray et al*., 2008). *Reproduced with permission from Elsevier*.

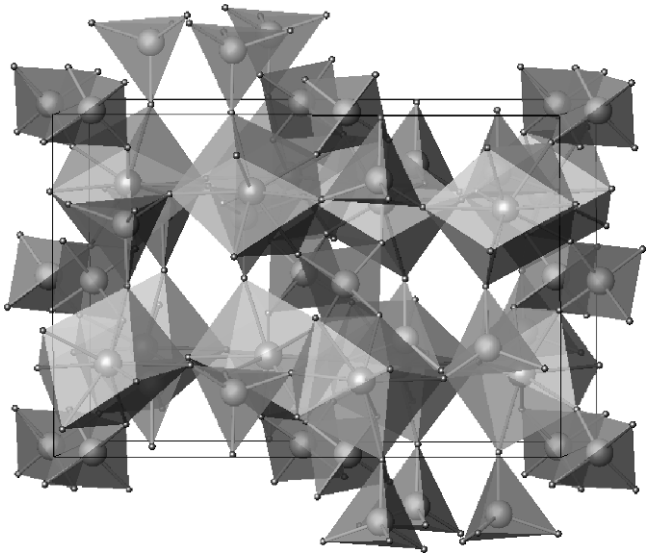

Fig. 39.12 *Three-dimensional framework of* UO_8 *square antiprisms and* MoO_4 *tetrahedra in the structure of* γ-UMo_2O_8.

polyhedra share common anions to form a three-dimensional framework. It is of interest that γ-UMo_2O_8 is isostructural to its Pu(IV) analog, $PuMo_2O_8$, and to UW_2O_8 and β-ThW_2O_8.

39.5 STRUCTURAL CHEMISTRY OF SELECTED An(V) (An = U, Np, Pu) COMPOUNDS

Hydrothermal synthesis of An(V) compounds has focused largely on neptunium, with only three structures reported for uranium and none for plutonium.

Pentavalent actinides most often occur in structures as part of approximately linear actinyl ions, in which the actinide cation is strongly bonded to two O atoms. These actinyl ions are then coordinated by from four to six ligands that are arranged at the equatorial vertices of square, pentagonal and hexagonal bipyramids. The bipyramids are capped by the actinyl O atoms.

In An(V) compounds, it is common for one or both of the O atoms of the actinyl ions to also be an equatorial ligand of an adjacent actinyl bipyramid (Fig. 39.13). This particular type of linkage has been termed a *cation–cation interaction* (Sullivan *et al.*, 1961; Grigoriev *et al.*, 1988, 1989a, b, 1993a, b; Albrecht-Schmitt *et al.*, 2003; Krot and Grigoriev, 2004; Sullens *et al.*, 2004; Alekseev *et al.*, 2007; Almond *et al.*, 2007; Forbes *et al.*, 2007) and has significant ramifications for structural connectivities. Cation–cation interactions are rare in An(VI) structures, where they occur in less than 2% of reported structures (Burns, 2005). Although An(VI) coordination polyhedra are geometrically similar to those of An(V), the prevalence of cation–cation interactions in An(V) materials leads to a substantial divergence of the structural topologies of An(V) compounds from those of An(VI). Krot and Grigoriev (2004) examined the ramifications of cation–cation interactions in An(V) compounds published prior to 2001.

Forbes and Burns (2007) considered the graphical representation of Np(V) structures containing cation–cation interactions, and provided some useful terminology for these interactions. The cation–cation interaction occurs through an O atom that is part of an actinyl ion that is designated the *donor* of the interaction. This O atom is also an equatorial ligand of a second actinyl polyhedron, where it coordinates an actinyl ion that is designated the *acceptor* of the cation–cation interaction. Whereas a given actinyl ion can only donate at

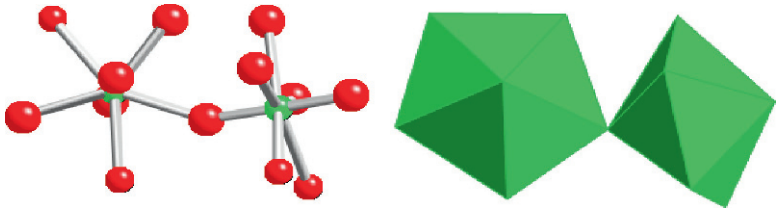

Fig. 39.13 *A cation–cation interaction in which an actinyl ion O atom is also an equatorial ligand of a bipyramid about another actinyl ion* (*ball-and-stick and polyhedral representations*).

most two cation–cation interactions, an actinyl ion can in principle accept as many as six cation–cation interactions.

The importance of hydrothermal synthesis for the preparation of Np(V) materials containing cation–cation appears to be substantial. Although some compounds containing these interactions have been produced under ambient conditions, the strong majority of inorganic Np(V) structures with cation–cation interactions were produced hydrothermally. Hydrothermal treatment appears to be even more important for the formation of Np(V) framework structures with cation–cation interactions, as all the known examples were produced hydrothermally.

Forbes *et al.* (2008) developed a structural hierarchy of inorganic neptunyl compounds that is dominated by Np(V) structures. This study provided revised bond-valence parameters for Np(V)–O interactions, average polyhedral geometries, and illustrations of the structural units in 43 Np(V) compounds. The hierarchy is based upon the linkages of the polyhedra containing higher valence cations into structural units that are finite clusters, chains, sheets, and frameworks. The known compounds are mostly distributed over the chain, sheet and framework classes, with some preference for sheets. Where cation–cation interactions between neptunyl polyhedra are present, there is a strong preference for frameworks of polyhedra. Forbes *et al.* (2008) found that the structures of Np(V) compounds that lacked cation–cation interactions have structural units that are topologically similar or identical to those in U(VI) compounds. Where cation–cation interactions occur in Np(V) compounds, new structural topologies usually result.

Most Np(V) compounds that contain structural chains were produced by evaporation of aqueous solutions at room temperature. Several of these solutions had been pre-treated hydrothermally, but this treatment did not produce crystals directly. The degree to which the hydrothermal pre-treatment impacted the outcome of the later evaporation-driven crystal growth is unclear. We examine here examples of such chains.

In inorganic Np(V) compounds, nine distinct chain topologies are known (Forbes *et al.*, 2008). Five of them lack cation–cation interactions and have topologies that are similar or identical to those known for U(VI) phases. An interesting example occurs in the structures of $Co(NH_3)_6(NpO_2)(SO_4)_2(H_2O)_2$ (Grigoriev *et al.*, 1991), $Na_3(NpO_2)(SO_4)_2(H_2O)_{2.5}$ (Forbes and Burns, 2005) and $CaZn_2(NpO_2)_2(SO_4)_4(H_2O)_{10}$ (Forbes and Burns, 2005) and is shown in Fig. 39.14a. The chain consists of neptunyl pentagonal bipyramids with one bidentate sulfate tetrahedron and three monodentate tetrahedra. The monodentate tetrahedra share vertices with three bipyramids, creating a chain with alternating bipyramids and tetrahedra. U(VI) uranyl sulfate chains with identical topologies have been reported in a hybrid organic–inorganic compound (Norquist *et al.*, 2003a, b).

The chain that is the basis of the structure of $Cs(NpO_2)(CrO_4)(H_2O)(H_2O)$ (Grigoriev *et al.*, 1995) has neptunyl pentagonal bipyramids that share edges,

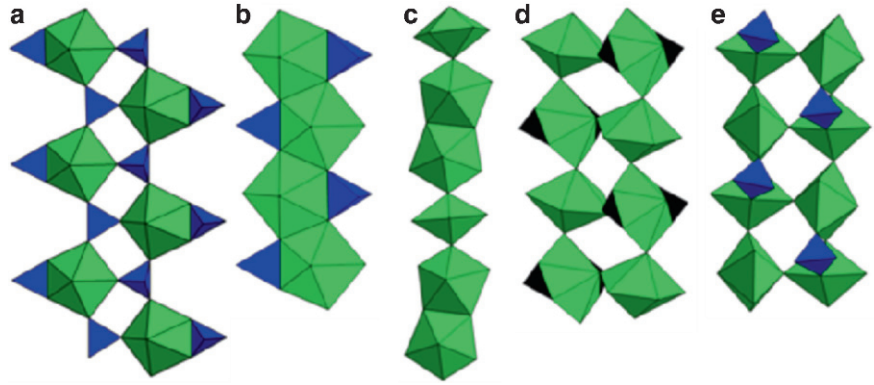

Fig. 39.14 *Polyhedral representations of chains of polyhedra that contain Np(V). Np(V) polyhedra are shown in green (adapted Forbes et al., 2008). Reproduced with permission from the American Chemical Society.*

with chromate tetrahedra located on either side where one of their edges is also an equatorial edge of a bipyramid (Fig. 39.14b). This chain topology is known from many U(VI) uranyl compounds, but in all cases the chains occur as part of a two-dimensional sheet that is based upon the uranophane or haiweeite anion topologies (Burns, 2005).

Four of the chains found in Np(V) compounds include cation–cation interactions, and most of these compounds were crystallized at room temperature. The structure of $K_4(NpO_2)_3Cl_7(H_2O)_4$ contains an interesting chain of neptunyl pentagonal bipyramids (Forbes and Burns, 2007). It has pairs of bipyramids that share an equatorial edge, with their neptunyl ions oriented approximately perpendicular to the chain length (Fig. 39.14c). A third bipyramid is located between these dimers along the chain length, where its neptunyl ion donates cation–cation interactions that are accepted by dimers on either side. Vertices of the pentagonal bipyramids that are not shared within the chains are occupied by either H_2O or Cl.

The chains that occur in the structures of $(NpO_2)_2(NO_3)_2(H_2O)_5$ and $(NpO_2)_2(SO_4)(H_2O)_6$ (Grigoriev *et al.*, 1994; Charushnikova *et al.*, 2006) have neptunyl pentagonal bipyramids and are two bipyramids wide. There are two types of neptunyl ions. One donates two cation–cation interactions while it accepts only one, and the other donates one cation–cation interaction and accepts two. The result is a chain in which cation–cation interactions form four-membered circuits (Fig. 39.14d, e). In one structure, equatorial vertices of the bipyramids that are not shared with other bipyramids are part of an edge that is shared with a nitrate triangle (Fig. 39.14d). In the other, sulfate tetrahedra bridge adjacent bipyramids along the chain length by sharing single vertices with adjacent bipyramids (Fig. 39.14e).

Three Np(V) compounds that are based upon sheets of polyhedra have been acquired through hydrothermal methods (Albrecht-Schmitt *et al.*, 2003; Forbes

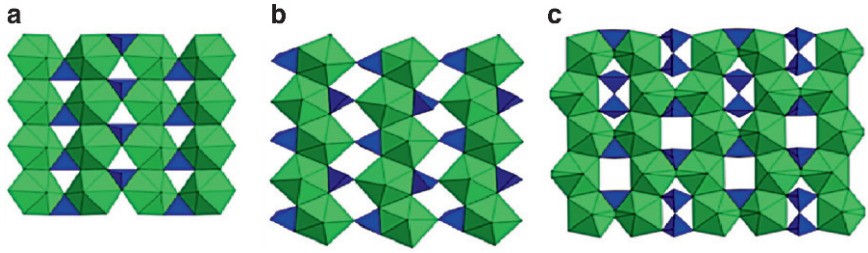

Fig. 39.15 *Sheets containing Np(V) neptunyl polyhedra* (*Forbes et al.*, 2008).

and Burns, 2006, 2009). The first of these was α-$Ag(NpO_2)(SeO_3)$, which was grown by heating to 180°C (Albrecht-Schmitt *et al.*, 2003). It contains a sheet that consists of edge-sharing Np(V) hexagonal bipyramids (Fig. 39.15a) that is based upon the rutherfordine sheet anion topology (Burns, 2005). Triangles in the anion topology are occupied by SeO_3 pyramids. A topologically identical sheet occurs in $[(UO_2)(SeO_3)]$, which has no interlayer constituents (Loopstra and Brandenburg, 1978).

The structure of $Ba(NpO_2)(PO_4)(H_2O)$ (Forbes and Burns, 2006), which was grown at 150°C, contains sheets of Np(V) pentagonal bipyramids and phosphate tetrahedra (Fig. 39.15b). The bipyramids share equatorial edges, forming a chain that is one polyhedron wide. The chains are linked into a sheet by sharing equatorial edges and vertices with phosphate tetrahedra. These sheets are topologically identical to U(VI) uranyl silicate sheets found in minerals and U(VI) uranyl phosphate sheets in hydrothermally synthesized compounds (Burns, 2005).

The first Np(V) silicate, $Li_6(NpO_2)_4(H_2Si_2O_7)(HSiO_4)_2(H_2O)_2$ was created by hydrothermal synthesis at 200°C (Forbes and Burns, 2008). It contains sheets of Np(V) pentagonal bipyramids and silicate tetrahedra (Fig. 39.15c). The bipyramids share equatorial edges, giving chains that are linked into a sheet by sharing select equatorial vertices. Sorosilicate and nesosilicate groups occur within the voids of the sheet of bipyramids.

A highly interesting sheet of neptunyl pentagonal bipyramids with cation–cation interactions was reported for the structure of $(NpO_2)Cl(H_2O)$ (Grigoriev *et al.*, 1993a, b). This compound was crystallized at room temperature. The sheet consists only of neptunyl pentagonal bipyramids in which each neptunyl ion donates two cation–cation interactions, as well as accepting two cation–cation interactions. This mode of connectivity results in a cationic net according to the terminology of Grigoriev *et al.* (1993a). In $(NpO_2)Cl(H_2O)$ the unshared equatorial ligands of the bipyramids are occupied by Cl. The compound $(NpO_2)_2(SO_4)(H_2O)_4$ has a similar cationic net of neptunyl pentagonal bipyramids (Forbes and Burns, 2009), but here sulfate tetrahedra bridge adjacent bipyramids. This compound was crystallized at room temperature following a hydrothermal pretreatment of the solution (Fig. 39.16).

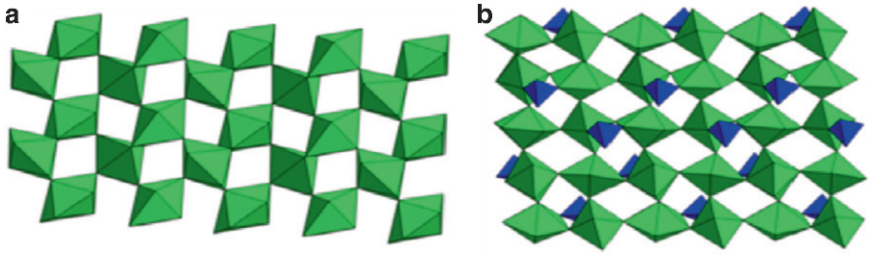

Fig. 39.16 *Polyhedral representations of sheets that occur in* $(NpO_2)Cl(H_2O)$ (a) (*Grigoriev et al.*, 1993a) *and* $(NpO_2)_2(SO_4)(H_2O)_4$ (*Forbes and Burns*, 2009) (b).

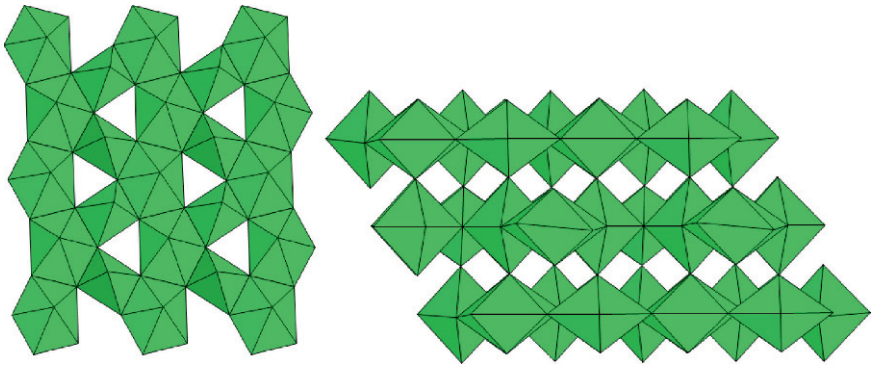

Fig. 39.17 *Polyhedral representations of the structure of* Np_2O_5 (*adapted from Forbes et al.*, 2008).

Frameworks are an important class of Np(V) compounds, and hydrothermal synthesis is proving to be an effective means to produce frameworks containing cation–cation interactions between Np(V) neptunyl ions.

Despite its simple chemical composition, the structure of Np_2O_5 was only reported in 2007 based upon a study of hydrothermally produced crystals (Forbes *et al.*, 2007). Other synthesis methods exist for Np_2O_5, but none have given crystals suitable for crystal structure analysis. Even the hydrothermal approach resulted in crystals of less than desirable quality, as they were both very small and twinned. The structure contains both Np(V) square and pentagonal bipyramids (Fig. 39.17). Although the bonding in all three dimensions is of similar strengths and importance, the structure has a pronounced layering. These layers consist of chains formed by the sharing of edges between pentagonal bipyramids, with the chains linked into the layer by the sharing of edges between square bipyramids and the pentagonal bipyramids of the chains. Despite the fact that the layer is based on the well-known uranophane anion topology, it is highly unusual in that the neptunyl ions within the square bipyramids are oriented roughly parallel with the plane of the layer, and both

of the O atoms of the neptunyl ion donate cation–cation interactions that are accepted by neptunyl ions within pentagonal bipyramids of the chains. The layers are stacked in the third dimension, and are strongly linked together through cation–cation interactions that are donated by the neptunyl ions in the pentagonal bipyramids of one layer, and are accepted by the square bipyramidal neptunyl ions in the adjacent layer.

The compound $Na[NpO_2(OH)_2]$ is an interesting example of a framework structure that formed during a hydrothermal reaction (Almond *et al.*, 2007). The structure (Fig. 39.18) consists of chains of equatorial-edge-sharing neptunyl pentagonal bipyramids that are stitched into a framework by cation–cation interactions that extend between chains. The Na cations are located in voids within this framework. The presence of cation–cation interactions creates a framework with a connectivity that is elegantly simple but lacking in structures containing An(VI) cations.

It has been proposed that cation-cation interactions in neptunyl compounds may provide a super-exchange pathway that facilitates magnetic ordering (Jobiliong *et al.*, 2004; Almond *et al.*, 2007; Forbes *et al.*, 2006, 2007). Hydrothermal synthesis have provided material of sufficient quantity and quality for measurement of the magnetic properties of several Np(V) compounds. In the case of Np_2O_5, antiferromagnetic ordering was observed at 22 K (Forbes *et al.*, 2007), and in $Na[NpO_2(OH)_2]$ antiferromagnetic ordering occurred at 19.5 K (Almond *et al.*, 2007). Ferromagnetic ordering occurs in β-$AgNpO_2(SeO_3)$ at 7 K (Jobiliong *et al.*, 2004).

Whereas U(V) coordination compounds have received a great deal of attention in recent years, these are not produced hydrothermally. Generally, U(V) in solution disproportionates to U(IV) and U(VI) rapidly, precluding formation of U(V) compounds by hydrothermal synthesis. However, three studies have

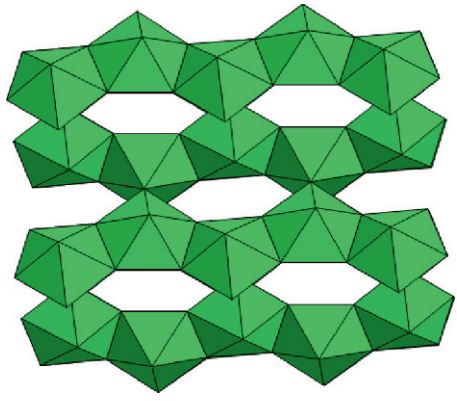

Fig. 39.18 *Polyhedral representation of the framework of Np(V) polyhedra that occur in the structure of* $Na[NpO_2(OH)_2]$ (*Forbes et al.*, 2008).

reported synthesis of novel U(V) compounds hydrothermally (Chen *et al.*, 2005; Belai *et al.*, 2008; Lin *et al.*, 2008).;

Two U(V) silicates and a U(V) germanate were produced by hydrothermal synthesis at the unusually high temperature of 600 °C (Chen *et al.*, 2005; Lin *et al.*, 2008). The first U(V) compound to be synthesized using a hydrothermal method was $K(UO)Si_2O_6$ (Chen *et al.*, 2005) which consists of a framework of U(V) square bipyramids and silica tetrahedra (Fig. 39.19). The square bipyramids consist of four long bonds ($\sim$ 2.16 Å) and two shorter bonds ($\sim$ 2.06 Å), thus no uranyl ion is present. The square bipyramids share a vertex, forming a chain that is one bipyramid wide. These chains are linked into a framework by sharing vertices with four-membered rings of silicate tetrahedra. The authors of this study proposed that water itself in the hydrothermal reaction is the reducing agent that resulted in U(V), as UO_3 was the only source of uranium in the reaction.

The isostructural compounds $K_3(U_3O_6)(Si_2O_7)$ and $Rb_3(U_3O_6)(Ge_2O_7)$ were also produced from hydrothermal synthesis at 600°C, where the source for U(V) was UO_3 (Lin *et al.*, 2008). The structures contain square bipyramids that are distorted into relatively short ($\sim$ 2.09 Å) to longer distances ($\sim$ 2.19 Å). The bipyramids share a vertex, forming a chain that is one bipyramid wide. These chains are linked through sharing vertices with other chains, giving a column of bipyramids that consists of three individual chains (Fig. 39.20). These columns are linked by the sharing of bipyramid vertices with silicate tetrahedra that themselves are present as Si_2O_7 sorosilicate units.

The mixed-valence compound $[U^{V}(H_2O)_2(U^{VI}O_2)_2O_4(OH)](H_2O)_4$ was produced hydrothermally at 120°C by reacting uranyl acetate, zinc metal, and hydrazine (Belai *et al.*, 2008). The structure of this compound consists of sheets

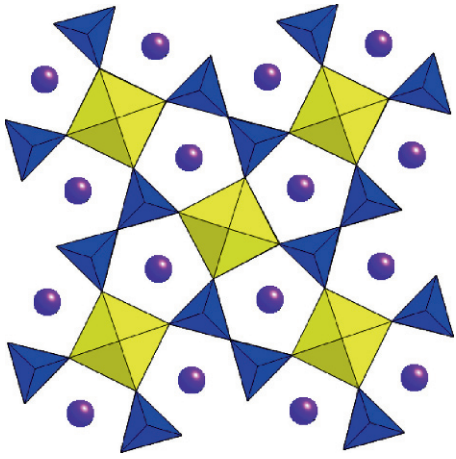

Fig. 39.19 *Polyhedral representation of the structure of $K(UO)Si_2O_6$. U(V) polyhedra are shown in yellow, with silicate tetrahedra in blue.*

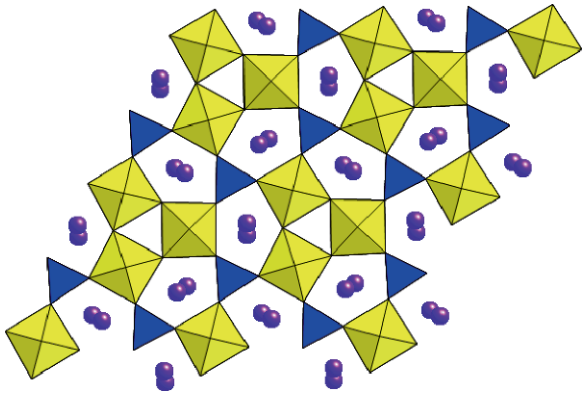

Fig. 39.20 *Polyhedral representation of the crystal structure of* $K_3(U_3O_6)(Si_2O_7)$. *U(V) polyhedra are shown in yellow and silicate tetrahedra are colored blue.*

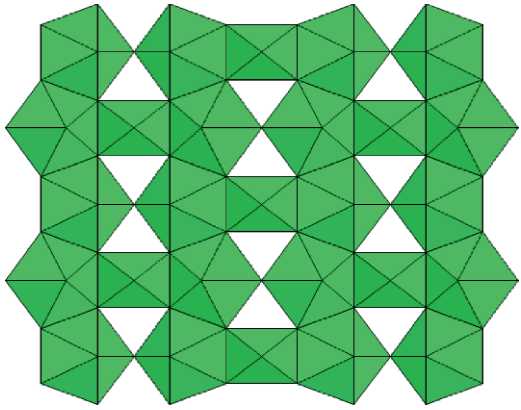

Fig. 39.21 *Polyhedral representation of the structure of* $U^V(H_2O)_2(U^{VI}O_2)_2O_4(OH)](H_2O)_4$. *U(V) square bipyramids and U(VI) pentagonal bipyramids are shown in green.*

of U(VI) uranyl pentagonal bipyramids and U(V) square bipyramids (Fig. 39.21). The square bipyramids consist of four short (~ 2.06 Å) and two long (~ 2.42 Å) bonds. Pentagonal bipyramids share an equatorial edge with pentagonal bipyramids on two sides, resulting in a chain that is one bipyramid wide. These chains are linked into a sheet by the sharing of equatorial vertices between every third pentagonal bipyramid along the chain length on either side. The square bipyramids are positioned between the chains of pentagonal bipyramids, where they share two equatorial edges with pentagonal bipyramids. This structural sheet bears resemblance to those found in the mixed-valence U(V)-U(VI) carbonate minerals wyartite (Burns and Finch, 1999) and dehydrated wyartite (Hawthorne *et al.* 2006), as well as to other minerals based on the β-U_3O_8 sheet anion topology (Burns, 2005).

39.6 STRUCTURAL CHEMISTRY OF An(VI) (An = U, Np, Pu) COMPOUNDS

Most of the hydrothermally prepared An(VI) compounds contain linear actinyl ions, $An(VI)O_2^{2+}$, which determines their structural chemistry. An(VI) salts containing tetrahedral and pseudo-tetrahedral oxoanions TO_n (n = 3, 4; T = S, P, Mo, Cr, W, Se, As, etc.) are the most studied in the literature. Here we shall concentrate on structural chemistry of actinyl molybdates, selenates and sulfates as an example of rich structural diversity that may provide important insight into the self-assembly mechanisms. Fedosseev *et al.* (1998) investigated complex formation of hexavalent Np and Pu with tetrahedral TO_4 oxoanions (T = S, Se, Cr, Mo) in aqueous solutions. They demonstrated that most of the Np(VI) and Pu(VI) compounds prepared are either isostructural to their U(VI) counterparts or possess structural units typical to similar U(VI) salts. For instance, $Na_2(NpO_2)(MoO_4)_2{\cdot}4H_2O$ is isostructural to its uranium analog, whereas isotypic $K_2(PuO_2)_2(CrO_4)_3{\cdot}4H_2O$ and $K_2(NpO_2)_2(CrO_4)_3{\cdot}4H_2O$ are based upon $[(NpO_2)_2(CrO_4)_3(H_2O)]$ sheets topologically identical to the sheets observed in a series of amine-templated uranyl selenates (Krivovichev *et al.*, 2006, 2009). Thus, in the following we shall discuss some aspects of structural chemistry of hydrothermally prepared An(VI) compounds using uranyl compounds as the most detailed characterized system.

A wide range of uranyl molybdates have been prepared hydrothermally at temperatures ranging from 100°C to 220°C. In most cases, the uranyl cation is coordinated by five additional anions that results in formation of a pentagonal bipyramid, whereas Mo(VI) atoms usually possess tetrahedral coordination. The U(VI) and Mo(VI) polyhedra share common anions to form structural units of various topologies and dimensionalities. Figure 39.22 shows uranyl molybdate complexes observed in compounds formed in the Na–Tl–U–Mo–H_2O system at 120°C or 180°C (Krivovichev and Burns, 2003). The structure of $Na_3Tl_3[(UO_2)(MoO_4)_4]$ is based upon a finite branched-4-membered ring (4-MR) cluster with composition $[(UO_2)_2(MoO_4)_8]$ (Fig. 39.22a) that contains two UO_7 pentagonal bipyramids and eight MoO_4 tetrahedra. The structures of $Na_{13-x}Tl_{3+x}[(UO_2)(MoO_4)_3]_4(H_2O)_{6+x}$ (x = 0.1) and $Na_3Tl_5[(UO_2)(MoO_4)_3]_2(H_2O)_3$ are based on one-dimensional chains of composition $[(UO_2)(MoO_4)_3]$ (Figs. 39.22c–f). The structure of $Na_2[(UO_2)(MoO_4)_2](H_2O)_4$ (which is isotypic to its Np(VI) analog) is based upon 2-D units of composition $[(UO_2)(MoO_4)_2]$ (Fig. 39.22h). Figure 39.22b, g, and i shows black-and-white graphs that describe topology of linkage of coordination polyhedra in corresponding finite cluster, chain and sheet, respectively (here black and white nodes symbolize U and Mo polyhedra, respectively). It is noteworthy that all three uranyl molybdate complexes contain 4-membered rings (4-MRs) as their basic building unit.

Grigoriev *et al.* (2003) reported the structure of mixed-valence Np(V)–Np(VI) molybdate, $Na_6[(Np^{V}O_2)_2(Np^{VI}O_2)(MoO_4)_5]{\cdot}13H_2O$ and noted that the isotypic Np(V)–U(VI) mixed-actinide compound $Na_6[(Np^{V}O_2)_2(U^{VI}O_2)$

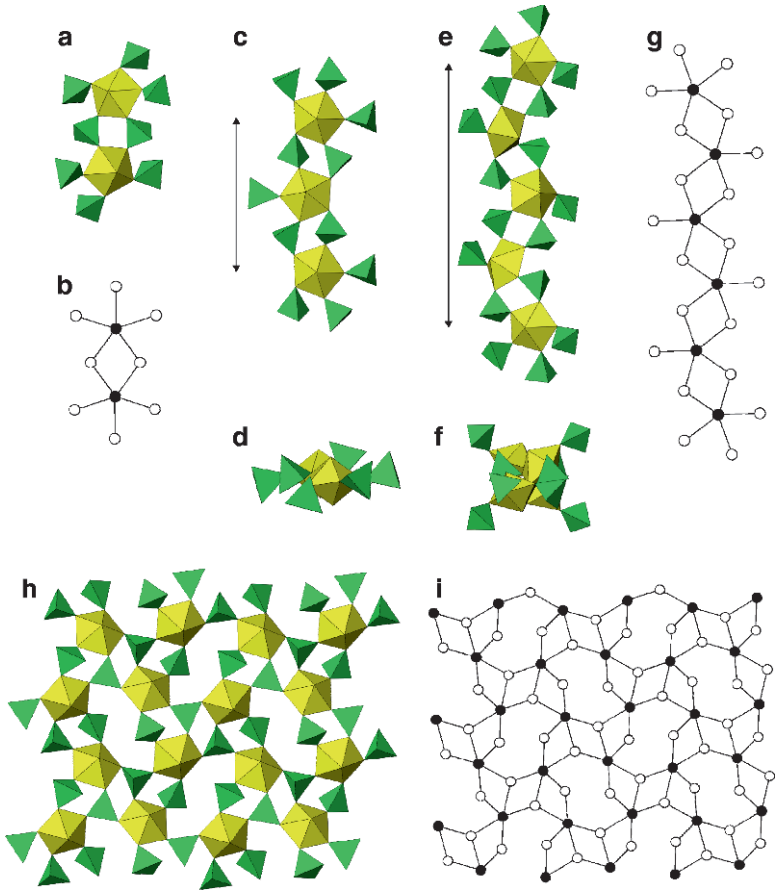

Fig. 39.22 *Uranyl molybdate complexes formed as a result of hydrothermal reactions in the Na–Tl–U–Mo–H_2O system at* 120°*C or* 180°*C* (*adapted from Krivovichev and Burns*, 2003).

$(MoO_4)_5]\cdot 13H_2O$ has been prepared as well. The structure of the Np(V)–Np(VI) compound contains 2-D sheets formed by corner sharing between NpO_7 pentagonal bipyramids and MoO_4 tetrahedra (Fig. 39.23). A similar topology has also been observed in analogous uranyl compounds – amine-templated molybdate $(NH_3(CH_2)_3NH_3)(H_3O)_2[(UO_2)_3(MoO_4)_5]$ (Halasyamani *et al*. 1999) and inorganic uranyl selenates $M_2[(UO_2)_3(SeO_4)_5](H_2O)_{16}$ (M = Mg, Co, Zn) (adapted from Krivovichev and Kahlenberg, 2004, 2005a).

The structural chemistry of hydrothermal uranyl molybdates is extremely diverse and its full description is beyond the topic of this chapter (a systematic survey can be found in Krivovichev and Burns (2008)). Of particular interest is the propensity of uranyl molybdates to form microporous frameworks in

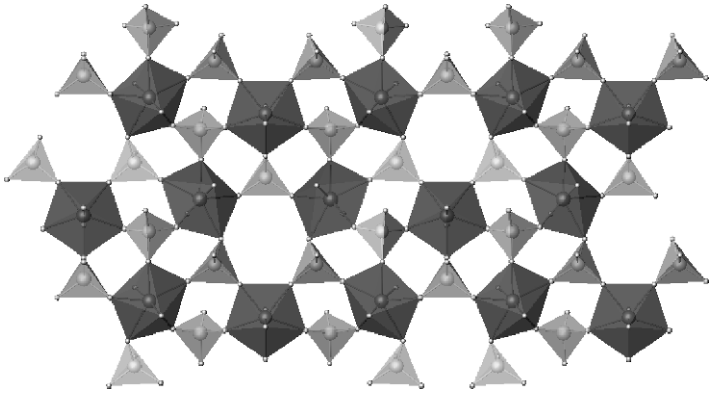

Fig. 39.23 *Neptunyl molybdate sheet in* $Na_6[(Np^{V}O_2)_2(Np^{VI}O_2)(MoO_4)_5]\cdot 13H_2O$.

the course of hydrothermal reactions. An interesting example is the series of chiral microporous compounds consisting of 3-D frameworks with general formula $[(UO_2)_n(MoO_4)_m(H_2O)_l]$. There are three topological types of chiral frameworks known with the n:m ratio of 6:7, 5:7, and 4:5. The 6:7 frameworks have been first identified by Tabachenko *et al.* (1984) in the structures of $M(UO_2)_6(MoO_4)_7(H_2O)_{14}$ (M = Mg, Sr) that crystallize in orthorhombic $C222_1$ space group. Later compounds with this framework type have been prepared hydrothermally in the presence of amines that play a role of guest molecules in the framework cavities (Krivovichev *et al.*, 2005a, b, c). It is also of interest that the isotypic uranyl sulfate framework with the 6:7 ratio had been reported (Doran *et al.*, 2002). The structure of the only known 5:7 compound, $(NH_4)_4[(UO_2)_5(MoO_4)_7](H_2O)_5$ (Krivovichev *et al.*, 2003), consists of a three-dimensional framework of composition $[(UO_2)_5(MoO_4)_7]^{4-}$ (Fig. 39.24).

The framework contains a three-dimensional system of channels. The largest channel is parallel to [001] and has the dimensions 7.5 × 7.5 Å, which results in a crystallographic free diameter (effective pore width) of 4.8 × 4.8 Å (based on an oxygen radius of 1.35 Å). Smaller channels extend parallel to [100], [110], [010], [−110], [1–10] and [−1–10] and have dimensions 5.2 × 6.3 Å (giving an effective pore width of 2.5 × 3.6 Å). Four symmetrically unique NH_4^+ cations and H_2O molecules are located in the framework channels. The $[(UO_2)_5(MoO_4)_7]^{4-}$ framework is unusually complex. Its nodal representation is shown in Fig. 39.24b. Each node corresponds to a UO_7 bipyramid (black) or a MoO_4 tetrahedron (white). All black vertices are five-connected and all white vertices are either three- or four-connected. Using the nodal representation, the uranyl molybdate framework in the structure of $(NH_4)_4[(UO_2)_5(MoO_4)_7](H_2O)_5$ can be described in terms of fundamental chains. The nodal representation of the fundamental chain corresponding to the uranyl molybdate framework is shown in Fig. 39.24c. The chain is a sequence of three- and four-connected MoO_4 tetra-

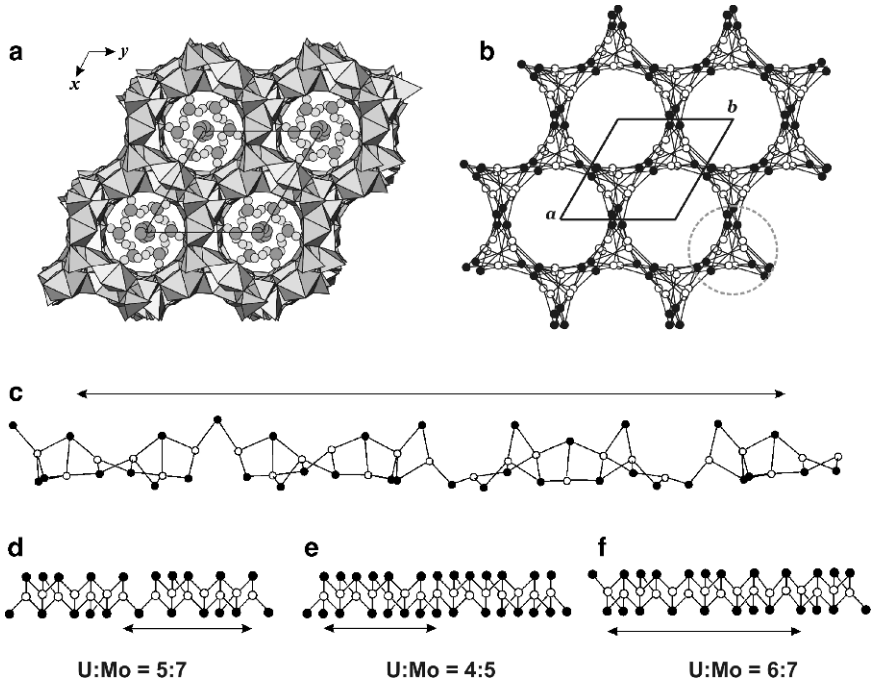

Fig. 39.24 *The structure of* $(NH_4)_4[(UO_2)_5(MoO_4)_7](H_2O)_5$ *projected along the c axis* (*a*), *nodal representation of its* $[(UO_2)_5(MoO_4)_7]$ *framework* (*b*), *nodal representation of its fundamental chain* (*c*), *and graphs isomorphous to nodal representations of fundamental chains of chiral uranyl molybdate frameworks with the U:Mo ratio of* 5:7, 4:5 *and* 6:7 (*d*, *e and f*, *respectively*) (*adapted from Krivovichev and Burns*, 2008). *Reproduced with permission from Elsevier*.

hedra (white vertices) linked through one, two or three UO_7 pentagonal bipyramids (black vertices). The graph shown in Fig. 39.24c can be further reduced to the simplified isomorphic graph shown in Fig. 39.24d. This reduction preserves all topological linkages between the nodes. Note that the graph shown in Fig. 39.24d is periodic and its identity unit includes seven white vertices, whereas, in the real structure, the identity period of the fundamental chain includes 21 white vertices. Thus the topological structure of the fundamental chain is simpler than its geometrical realization.

Distinction of a fundamental chain permits the comparison of the 5:7 uranyl molybdate framework in $(NH_4)_4[(UO_2)_5(MoO_4)_7](H_2O)$ with the 6:7 and 4:5 chiral uranyl molybdate frameworks. The two latter frameworks can also be described as based upon fundamental chains of UO_7 and MoO_4 polyhedra. The reduced graphs of these chains are shown in Figs. 39.24e and f for 4:5 and 6:7 frameworks, respectively. Detailed examination of these graphs demonstrated that they cannot be transformed one into another without significant topolog-

ical reconstruction. Thus, the fundamental chains that form bases for the chiral uranyl molybdate frameworks with U:Mo = 5:7, 4:5 and 6:7 are topologically different, though closely related. The observed topological relationships might be the result of the presence of similar building blocks in the aqueous solutions from which the compound crystallized. Therefore, it is of great interest – both from fundamental and practical viewpoints – to reveal those complexes that may serve as building units at the stage of self-assembly of different actinide-based structures.

The basic structural feature of hydrothermally prepared An(VI) molybdates, selenates, chromates, and some sulfates is formation of extended structural units by corner sharing between An(VI) polyhedra and TO_4 tetrahedra. A similar situation had been observed for open-framework metal phosphates, where a fundamental importance of 4-membered rings had been proposed (Taulelle *et al.*, 1999; Neeraj *et al.* 2000; Rao *et al.*, 2001). Usually, the structural information concerning self-assembly in transition metal phosphate hydrothermal solutions is derived from the observations of crystallization sequences and structural studies of intermediate and metastable phases. In aqueous chemistry of An(VI) compounds, an excellent example of appropriate system is provided by uranyl selenates. The aqueous uranyl selenate systems are especially attractive, since most of the compounds are soluble under ambient conditions and can be crystallized by isothermal evaporation. Though the process usually takes place under ambient conditions, similar mechanisms may be at work in hydrothermal systems as well.

Crystals of two modifications of $Mg_2[(UO_2)_3(SeO_4)_5](H_2O)_{16}$ have been prepared from aqueous solutions as reported by Krivovichev and Kahlenberg (2004). The initial solution was prepared by dissolution of MgO and uranyl nitrate in selenic acid. Formation of a large amount lamellar green crystals of β-$Mg_2[(UO_2)_3(SeO_4)_5](H_2O)_{16}$ can be observed in ca. 24 h. In parallel, small crystals of the α-phase formed as well. In 48 h, crystals of the β-phase dissolved completely and crystallization process ended with formation of the α-modification. Thus the metastability of the β-phase made its structural characterization difficult. The structures of both modifications are shown in Fig. 39.25. They are based upon 2-D sheets with the same composition $[(UO_2)_3(SeO_4)_5]$ (Fig. 39.26). Both sheets consist of 4- and 6-MRs formed by corner sharing between UO_7 bipyramids and SeO_4 tetrahedra. However, the topology of the arrangement of the rings is different for the two structures as can be seen from their nodal representations (Figs. 39.26c, d). Thus, the process of the transformation involves conservation of the structure elements with single 4-MR or association of 4-MRs playing a role of building blocks for the two structures.

The time-dependent phase formation in the 1,10-diaminodecane–UO_2SeO_4–H_2O system was investigated and two different phases have been obtained: $[C_{10}H_{26}N_2][(UO_2)(SeO_4)_2(H_2O)]$ $(H_2SeO_4)_{0.85}(H_2O)_2$ (**A**) and $[C_{10}H_{26}N_2]$ $[(UO_2)(SeO_4)_2]$ $(H_2SeO_4)_{0.50}(H_2O)$ (**B**) (Krivovichev *et al.*, 2007). The phase **A** formed first as yellow elongated plate-like crystals. In ca. 10 h, the crystals

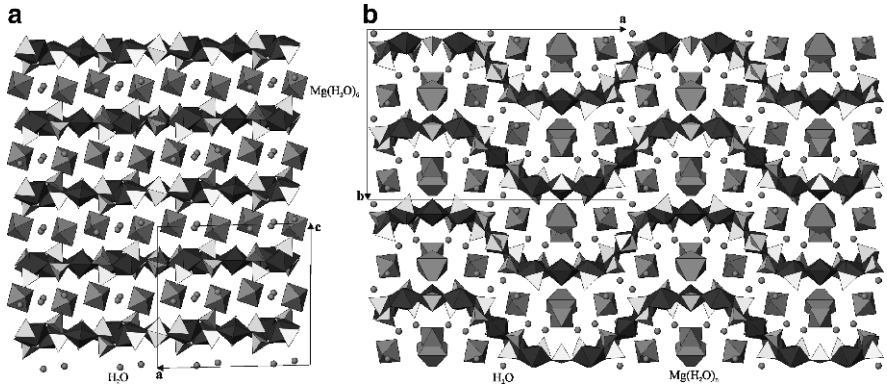

Fig. 39.25 *Structures of* α- (*a*) *and* β- (*b*) *modifications of* $Mg_2[(UO_2)_3(SeO_4)_5](H_2O)_{16}$ *viewed parallel to the extension of the uranyl selenate sheets* (*adapted from Krivovichev and Kahlenberg*, 2004).

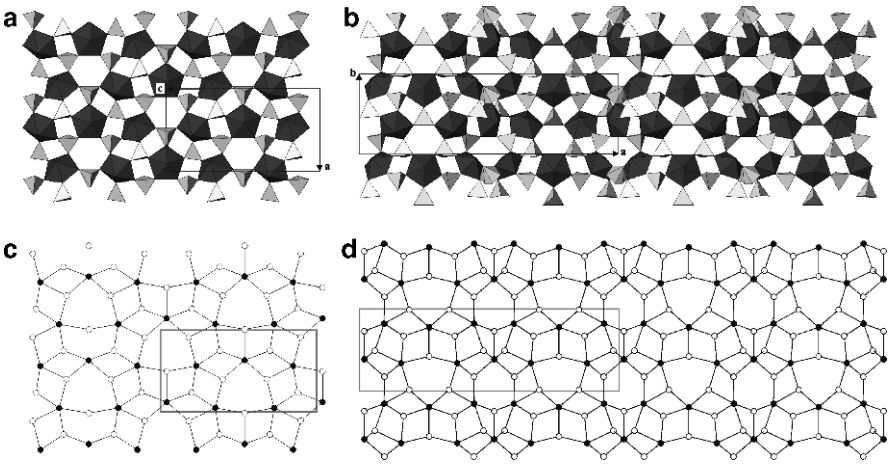

Fig. 39.26 *Polyhedral diagrams of uranyl selenate sheets in the structures of* α- (*a*) *and* β- (*b*) *modifications of* $Mg_2[(UO_2)_3(SeO_4)_5](H_2O)_{16}$, *and their nodal representations* (c and d, *respectively*) (*adapted from Krivovichev and Kahlenberg*, 2004). *Reproduced with permission from Wiley-VCH Verlag GmbH & Co.*

dissolved completely and a clear solution was observed with subsequent crystallization of the plates of the **B** phase. Figure 39.27 shows uranyl selenate complexes that constitute a basis for the two structures. The structural unit in the **A** phase is a 1-D chain, whereas that in the **B** phase is a 2-D sheet. Thus, the evaporation-induced process involved a 1-D/2-D transformation. This type of transformation has been repeatedly observed during hydrothermal crystalliza-

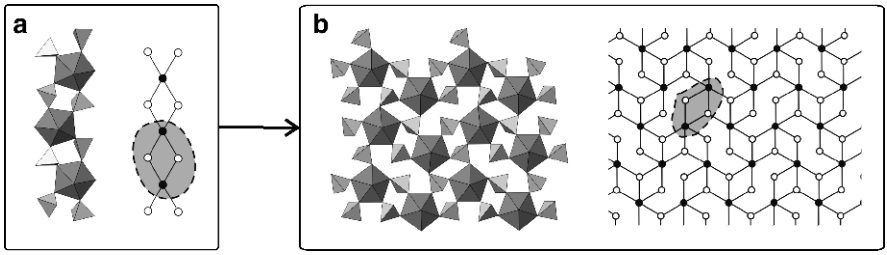

Fig. 39.27 1-*D*/2-*D phase transformation in the* 1,10-*diaminodecane–*UO_2SeO_4*–*H_2O *system: uranyl selenate chain in the* A *phase and its graph* (*a*) *and uranyl selenate sheet in the* B *phase and its graph* (*b*). *The* 4-*MR is highlighted in the two topologies.*

tion of metal phosphates (Francis *et al.*, 1997; Walton *et al.*, 2000, 2001; Choudhury *et al.*, 2001; Wang *et al.*, 2003).

Oliver *et al.* (1998) considered the aluminophosphate chain with topology identical to that shown in Fig. 39.27a as a prenucleation building block in hydrothermal Al-P chemistry. It is also noteworthy that the two topologies shown in Fig. 39.27 may be viewed as a result of condensation of 4-MRs. In metal phosphate chemistry, identification of a phase with cyclic 4-MR unit was considered as a proof of its crucial role as a building block in hydrothermal solutions (Neeraj *et al.*, 2000). A similar phase was also observed in uranyl selenate systems. Krivovichev and Kahlenberg (2005b) reported the structure of $[C_3H_{12}N_2][(UO_2)(SeO_4)_2(H_2O)_2](H_2O)$ that contains the branched 4-MR tetramer $[(UO_2)_2(SeO_4)_4(H_2O)_4]^{4-}$ (Fig. 39.28). One may suggest that units of this type play an essential role during formation and crystallization of An(VI) oxysalts under both ambient and hydrothermal conditions.

The An(VI) selenate, chromate, and molybdate compounds prepared under hydrothermal conditions demonstrate many structural similarities. In contrast, An(VI) sulfates are fundamentally different, since, in many cases, actinyl sulfate structural units are based upon bidentate An(VI) coordination, i.e. edge sharing between An(VI) bipyramids and SO_4 tetrahedra. Figure 39.29 shows 0-D and 1-D units with edge-sharing between An(VI) polyhedra and sulfate anions observed in hydrothermally synthesized An(VI) compounds. The simplest example is a sulfate analog of a tricarbonate cluster (Fig. 39.29a), which has been isolated in the structure of $[N_2C_5H_{14}]_2[UO_2(SO_4)_3]$ (Doran *et al.*, 2003). A monomer with one edge-sharing and three corner-sharing sulfate tetrahedra (Fig. 39.29b) attached to the An(VI) pentagonal bipyramid had been observed in a series of sodium and potassium uranyl sulfates crystallized from aqueous solutions at temperatures close to 70°C (Burns and Hayden, 2002; Hayden and Burns, 2002a, b).

Cyclic uranyl sulfate clusters shown in Fig. 39.29c and d were found in the structures of $K_4[UO_2(SO_4)_3]$ (Fig. 39.29c) (Mikhailov *et al.*, 1977), $[N_4C_6H_{22}]_2[(UO_2)_2(SO_4)_6](H_2O)$ (Norquist *et al.*, 2003a, b), and $[Co(NH_3)_6]$

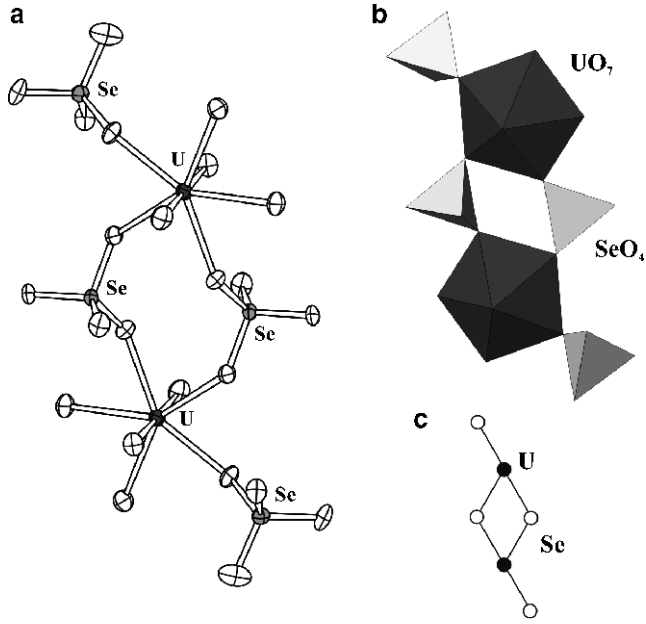

Fig. 39.28 *Possible prenucleation building unit in uranyl selenate systems: the* $[(UO_2)_2(SeO_4)_4(H_2O)_4]^{4-}$ *tetramer from the structure of* $[C_3H_{12}N_2][(UO_2)(SeO_4)_2(H_2O)_2](H_2O)$ *shown in displacement ellipsoids* (*a*), *polyhedral* (*b*) *and nodal* (*c*) *representations* (*adapted from Krivovichev and Kahlenberg*, 2005b)

$(H_8O_3)[NpO_2(SO_4)_3]$ (Grigoriev *et al.*, 1991). One-dimensional chains have been found in several amine-templated uranyl sulfates (Norquist *et al.*, 2003a, b) and $[Co(NH_3)_6][NpO_2(SO_4)_2](H_2O)_2$ (Grigoriev *et al.*, 1991). These examples obviously confirm structural similarities between U(VI) and Np(VI) compounds noticed by Fedosseev *et al.* (1998).

The presence of bidentate coordination of An(VI) by sulfate ion is in good agreement with the results of the U L_{III}-edge EXAFS measurements in aqueous solutions with excess of sulfate (Moll *et al.*, 2000; Hennig *et al.*, 2008).

The influence of fluoride ions upon uranyl sulfate chemistry under hydrothermal conditions was studied by Mikhailov *et al.* (2002) and Doran *et al.* (2005). In the structures of uranyl sulfate fluorides, F^- ions perform as bridging ligands between adjacent U(VI) centers. As a result, structural units contain a uranyl-fluoride substructure coordinated by sulfate anions (Fig. 39.30). So far, all uranyl sulfate fluorides possess layered structures with uranyl polyhedra forming fluoride-bridged chains (Fig. 39.30a, b, c) or tetramers (Fig. 39.30d). As a result, structural chemistries with and without fluorine in initial solution are dramatically different.

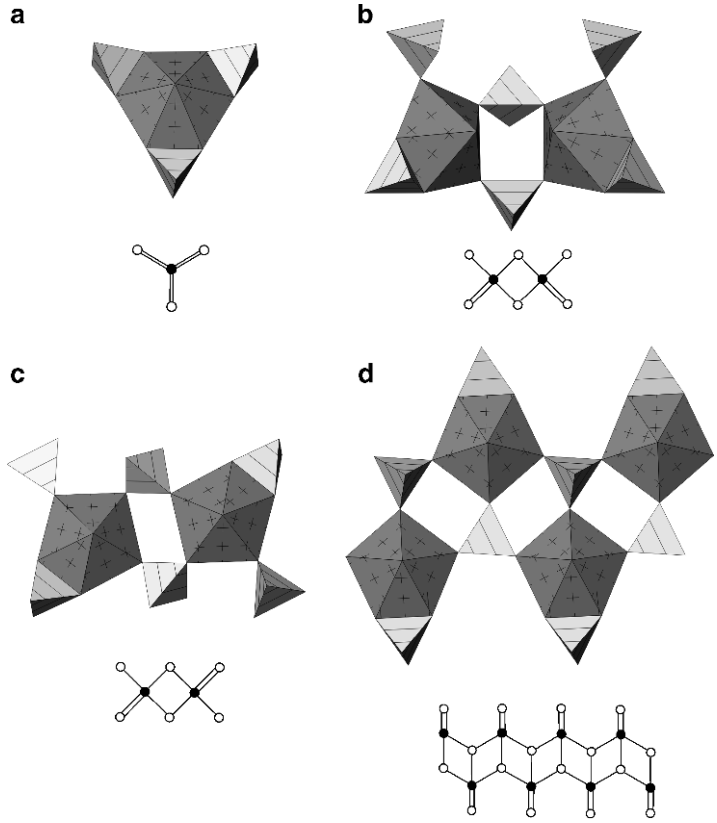

Fig. 39.29 *An(VI) sulfate clusters and* 1*-D chains in hydrothermally prepared An(VI) compounds* (*adapted from Krivovichev and Burns*, 2008). *Reproduced with permission from Elsevier*.

39.7 CONCLUSIONS AND PERSPECTIVES

Hydrothermal synthesis is clearly a synthetic method well-suited for preparing actinide compounds. Numerous novel structure types have been discovered, and the bonding in these compounds has yielded unusual physical properties that are aptly highlighted by long-range magnetic ordering in Np(V) compounds with cation–cation interactions. Other properties have been discovered from actinide phases derived from hydrothermal methods. These properties include selective ion-exchange, selective oxidation catalysis, photoluminescence, and intercalation. This chapter has focused primarily on oxoanion compounds, but more general solvothermal methods could be applied to the preparation of many other species not containing oxygen.

We are now seeing a shift away from merely trying to prepare uranyl compounds with new topologies to a concerted attempt to gain a deep understanding of the

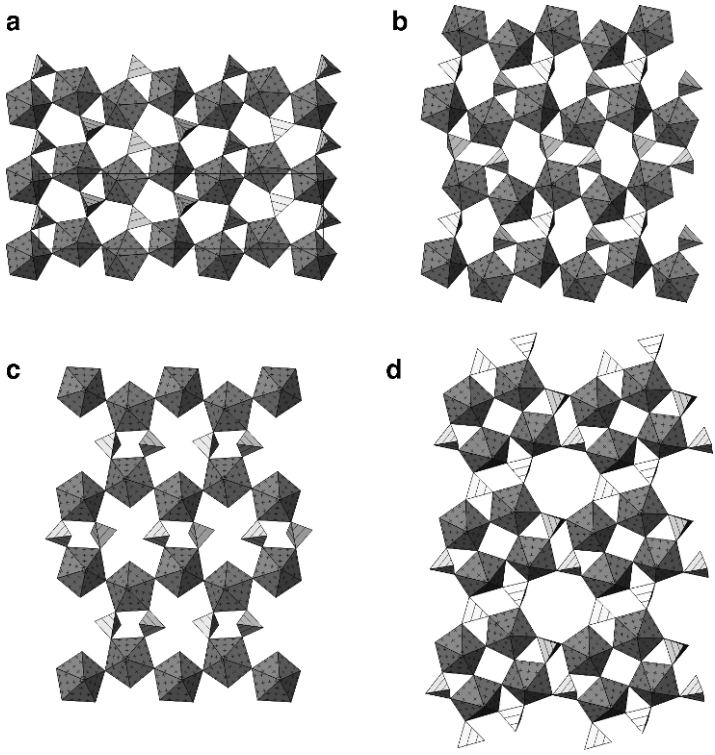

Fig. 39.30 *Uranyl fluoride sulfate sheets in* $Rb[UO_2(SO_4)F]$ (*a*), $[N_2C_3H_{12}][UO_2F(SO_4)]_2(H_2O)$ (*b*), $[N_2C_5H_{14}][UO_2F(H_2O)(SO_4)]_2$ (*c*), *and* $[N_2C_6H_{18}]_2[UO_2F(SO_4)]_4(H_2O)$ (*d*) (*adapted from Krivovichev and Burns*, 2008).

relationship between structures. These efforts are especially well-developed in magneto-structural correlations in Np(V) compounds. Furthermore, the hydrothermal transuranium chemistry that has been uncovered allows investigators to rationally prepare compounds in specific oxidation states. Judicious choice of ligands with specific geometries such as diphosphonates allows for the preparation of heterobimetallic mixed-actinide compounds containing actinides in two different oxidation states. As this field matures designed structures will become more common.

One area that is still lacking is in situ studies on redox processes with actinides, especially neptunium and plutonium, and in situ X-ray diffraction studies to understanding the kinetics and perhaps mechanism of crystal growth. This work is planned for the near future, and we should have a detailed understanding of the mechanisms and kinetics of hydrothermal chemistry in the next 5 years.

ACKNOWLEDGMENTS

This work was supported in part by the Chemical Sciences, Geosciences and Biosciences Division, Office of Basic Energy Sciences, Office of Science, Heavy Elements Program, U.S. Department of Energy, and by the Russian Ministry of Science and Education.

REFERENCES

Albrecht-Schmitt, T. E., Almond, P. M., and Sykora, R. E. (2003) *Inorg. Chem.*, **42**, 3788–95.

Alekseev, E. V., Krivovichev, S. V., Malcherek, T., and Depmeier, W. (2007) *Inorg. Chem.*, **46**, 8442–4.

Almond, P. M., Deakin, L., Porter, M. O., Mar, A., and Albrecht-Schmitt, T. E. (2000) *Chem. Mater.*, **12**, 3208–13.

Almond, P. M., Sykora, R. E., Skanthakumar, S., Soderholm, L., Albrecht-Schmitt, T. E. (2004) *Inorg. Chem*., **43**, 958–63.

Almond, P. M., Skanthakumar, S., Soderholm, L., and Burns, P. C. (2007) *Chem. Mater.*, **19**, 280–5.

Bard, A. J., Parsons, R., and Jordan, R., (eds.) (1985) *Standard Potentials in Aqueous Solutions*, Marcel Dekker, New York and Basel, 843 pp.

Bean, A. C., Peper, S. M., and Albrecht-Schmitt, T. E. (2001) *Chem. Mater.*, **13**, 1266–72.

Bean, A. C., Scott, B. L., Albrecht-Schmitt, T. E., and Runde, W. (2003) *Inorg. Chem.*, **42**, 5632–6.

Belai, N., Frisch, M., Ilton, E. S., Ravel, B., and Cahill, C. L. (2008) *Inorg. Chem.*, **47**, 10135–40.

Bray, T. H., Ling, J., Choi, E.-S., Brooks, J. S., Beitz, J. V., Sykora, R. E., Haire, R. G., Stanbury, D. M., and Albrecht-Schmitt, T. E. (2007a) *Inorg. Chem.*, **46**, 3663–8.

Bray, T. H., Nelson, A.-G. D., Jin, G. B., Haire, R. G., and Albrecht-Schmitt, T. E. (2007b) *Inorg. Chem.*, **46**, 10959–61.

Bray, T. H., Sullens, T. A., Shvareva, T. Y., Sykora, R. E., Haire, R. G., and Albrecht-Schmitt, T. E. (2007c) *J. Solid State Chem.*, **180**, 79–83.

Bray, T. H., Skanthakumar, S., Soderholm, L., Sykora, R. E., Haire, R. G., and Albrecht-Schmitt, T. E. (2008) *J. Solid State Chem*., **181**, 493–8.

Burns, P. C. and Finch, R. J. (1999) *Am. Mineral*., **84**, 1456–60

Burns, P. C. and Hayden, L. A. (2002). *Acta Crystallogr*., **58**, i121–i123.

Burns, P. C. (2005) *Can. Mineral.*, **43**, 1839–94.

Charushnikova, I. A., Krot, N. N., and Polyakova, I. N. (2006) *Crystallogr. Rep.*, **51**, 201–04.

Chen, C. S., Lee, S. F., and Lii, K. H., (2005) *J. Am. Chem. Soc*., **127**, 12208–09.

Choudhury, A., Neeraj, S., Natarajan, S., and Rao C. N. R. (2001). *J. Mater. Chem*., 1537–46.

Cromer, T. and Larson, A. C. (1956) *Acta Cryst.* **9**, 1015–8.

Cunningham, B. B. and Werner, L. B. (1949) *J. Am. Chem. Soc.*, **71**, 1521–8.

Delage, C., Carpy, A., H'Naïfi, A., and Goursolle, M. (1986) *Acta Cryst.*, **C42**, 1475–7.

Doran, M., Norquist, A. J., and O'Hare, D. (2002) *Chem. Commun*., 2946–7.

Doran, M. B., Norquist, A. J., and O'Hare, D. (2003) *Inorg. Chem.*, **42**, 6989–94.
Doran, M. B., Cockbain, B. E., and O'Hare, D. (2005) *Dalton Trans.*, 1774–80.
Fedosseev, A., Budantseva, N., Bessonov, A., Grigoriev, M., and Krupa, J. C. (1998) *J. Alloys Compd.*, **271–273**, 154–8.
Forbes, T. Z., Burns, P. C., Skanthakumar, S., and Soderholm, L. (2007) *J. Amer. Chem. Soc.*, **129**, 2760–61.
Forbes, T. Z., and Burns, P. C. (2007) *J. Solid State Chem.*, **180**, 106–12.
Forbes, T. Z. and Burns, P. C. (2005) *J. Solid State Chem.* **178**, 3445–52.
Forbes, T. Z. and Burns, P. C. (2006) *Am. Mineral.*, **91**, 1089–93.
Forbes, T. Z. and Burns, P. C. (2008) *Inorg. Chem.*, **47**, 705–12.
Forbes, T. Z., Wallace, C., and Burns, P. C. (2008) *Can. Mineral.*, **46**, 1623–45.
Forbes, T. Z., and Burns, P. C. (2009) *J. Solid State Chem.*, **182,** 43–8.
Forbes, T. Z., Burns, P. C., Soderholm, L., and Skanthakumar, S. (2006) *Chem. Mater.*, **18**, 1643–9.
Francis, R. J., Price, S. J., O'Brien, S., Fogg, A. M., O'Hare, D., Loiseau, T., and Férey, G. (1997). *Chem. Commun.*, 521–2.
Grigoriev, M. S., Yanovskii, A. I., Fedoseev, A. M., Budantseva, N. A., Struchkov, Y. T., Krot, N. N., and Spitsyn, V. I. (1988) *Doklady Akademii Nauk SSSR*, **300**, 618–22.
Grigoriev, M. S., Yanovskii, A. I., Struchkov, Y. T., Bessonov, A. A., Afonaseva, T. V., and Krot, N. N. (1989a) *Sov. Radiochem.*, **31**, 397–403.
Grigoriev, M. S., Yanovskii, A. I., Struchkov, Y. T., Bessonov, A. A., Afonas'eva, T. V., and Krot, N. N. (1989b) *Radiokhimiya*, **31**, 37–44.
Grigoriev, M. S., Fedoseev, A. M., Budantseva, N. A., Yanovskii, A. I., Struchkov, Yu. T., and Krot, N. N. (1991). *Radiokhimiya.*, **33**, 54–60.
Grigoriev, M. S., Bessonov, A. A., Krot, N. N., Yanovskii, A. I., and Struchkov, Y. T. (1993a) *Radiochemistry*, **35**, 382–7.
Grigoriev, M. S., Bessonov, A. A., Krot, N. N., Yanovskii, A. I., and Struchkov, Y. T. (1993b) *Radiokhimiya*, **35**, 17–23.
Grigoriev, M. S., Charushnikova, I. A., Krot, N. N., Yanovskii, A. I., and Struchkov, Y. T. (1994) *Zh. Neorgan. Khim.*, **39**, 179–83.
Grigoriev, M. S., Plotnikova, T. E., Baturin, N. A., Budantseva, N. A., and Fedoseev, A. M. (1995) *Radiokhimiya*, **37**, 102–05.
Grigoriev, M. S., Fedoseev, A. M., and Budantseva, N. A. (2003) *Russ. J. Coord. Chem.*, **29**, 877–9.
Halasyamani, P. S., Francis, R. J., Walker, S. M., and O'Hare, D. (1999). *Inorg. Chem.*, **38**, 271–9.
Hawthorne, F. C., Finch, R. J., and Ewing, R. C. (2006) *Can. Mineral.*, **44**, 1379–85.
Hayden, L. A. and Burns, P. C. (2002a) *Can. Mineral.*, **40**, 211–16.
Hayden, L. A. and Burns, P. C. (2002b) *J. Solid State Chem.*, **163**, 313–18.
Hennig, C., Ikeda, A., Schmeide, K., Brendler, V., Moll, H., Tsushima, S., Scheinost, A. C., Skanthakumar, S., Wilson, R., Soderholm, L., and Servaes, K. (2008). *Radiochim. Acta*, **96**, 607–11.
Jobiliong, E., Oshima, Y., Brooks, J. S., and Albrecht-Schmitt, T. E. (2004) *Solid State Commun.*, **132**, 337342.
Kolis, J. W. and Korzenski, M. B. (1999) *Chemical Synthesis Using Supercritical Fluids* (eds. P. G. Jessop and W. Leitner), Wiley-VCH, New York, pp. 213–41.
Krivovichev, S. V. and Burns, P. C. (2003). *Can. Mineral.*, **41**, 707–19.

Krivovichev, S. V. and Burns, P. C. (2004). *Dokl. Phys*., **49**, 76–7.
Krivovichev, S. V., Cahill, C. L., and Burns, P. C. (2003) *Inorg. Chem*., **42**, 2459–64.
Krivovichev, S. V. and Kahlenberg, V. (2004) *Z. Anorg. Allg. Chem*., **630**, 2736–42.
Krivovichev, S. V. and Kahlenberg, V. (2005a) *J. Alloys Compd*. **395**, 41–7.
Krivovichev, S. V. and Kahlenberg, V. (2005b) *Z. Anorg. Allg. Chem*., **631**, 2352–57.
Krivovichev, S. V., Cahill, C. L., Nazarchuk, E. V., Burns, P. C., Armbruster, T., and Depmeier, W. (2005a) *Micropor. Mesopor. Mater*., **78**, 209–15.
Krivovichev, S. V., Burns, P. C., Armbruster, T., Nazarchuk, E. V., and Depmeier, W. (2005b) *Micropor. Mesopor. Mater*., **78**, 217–24.
Krivovichev, S. V., Armbruster, T., Chernyshov, D. Yu., Burns, P. C., Nazarchuk, E. V., and Depmeier, W. (2005c) *Micropor. Mesopor. Mater*., **78**, 225–34.
Krivovichev, S. V., Gurzhiy, V. V., Tananaev, I. G., and Myasoedov, B. F. (2006) *Dokl. Phys. Chem*., **409**, 228–32.
Krivovichev, S. V., Burns, P. C., Tananaev, I. G., and Myasoedov, B. F. (2007) *J. Alloys Compd*., **444**–**445**: 457–63.
Krivovichev, S. V. and Burns, P. C. (2008) *Structural Chemistry of Inorganic Actinide Compounds* (eds. S. V. Krivovichev, P. C. Burns, I. G. Tananaev), Elsevier, Amsterdam, The Netherlands, pp. 95–182.
Krivovichev, S. V., Gurzhiy, V. V., Tananaev, I. G., and Myasoedov, B. F. (2009). *Z. Kristallogr*., in press.
Krot, N. N., and Grigoriev, M. S. (2004) *Uspekhi Khimii*, **73**, 94–106.
Lin, C. H., Chen, C. S., Shiryaev, A. A., Zubavichus, Y. V., and Lii, K. H. (2008) *Inorg. Chem.*, **47**, 4445–7.
Locock, A. J., Skanthakumar, S., Burns, P. C., and Soderholm, L. (2004) *Chem. Mater.*, **16**, 1384–90.
Loopstra, B. O. and Brandenburg, N. P. (1978) *Acta Crystallogr. B*, **34**, 1335–7.
Mikhailov, Yu. N., Kokh, L. A., Kuznetsov, V. G., Grevtseva, T. G., Sokol, S. K., and Ellert, G. V. (1977) *Koord. Khim*., **3**, 508–13.
Mikhailov, Yu. N., Gorbunova, Yu. E., Mit'kovskaya, E. V., Serezhkina, L. B., and Serezhkin, V. N. (2002) *Radiochem*istry, **44**, 315–18.
Moll, H., Reich, T., Hennig, C., Rossberg, A., Szabó, Z., and Grenthe, I. (2000). *Radiochim. Acta*, **88**, 559–66.
Morss, L. R., Edelstein, N. M., and Fuger, J. (2006) *The Chemistry of the Actinide and Transactinide Elements*, Springer, Dordrecht, The Netherlands, vol. 2, Chapter 6.
Neeraj, S., Natarajan, S., and Rao C. N. R. (2000) *J. Solid State Chem*., **150**, 417–22.
Nelson, A.-G. D., Bray, T. H., Zhan, W., Haire, R. G., and Albrecht-Schmitt, T. E. (2008a) *Inorg. Chem*., **47**, 4945–51.
Nelson, A.-G. D., Bray, T. H., and Albrecht-Schmitt, T. E. (2008b) *Angew. Chem.*, *Int. Ed.*, **47**, 6252–4.
Nelson, A.-G. D., Bray, T. H., Stanley, F. A., and Albrecht-Schmitt, T. E. (2009**)** *Inorg. Chem*., **48**, 4530–5.
Norquist, A. J., Doran, M. B., Thomas, P. M., and O'Hare, D. (2003a) *Dalton Trans*., 1168–75.
Norquist, A. J., Doran, M. B., Thomas, P. M., and O'Hare, D. (2003b) *Inorg. Chem*., **42**, 5949–53.
Oliver, S., Kuperman, A., and Ozin G. A. (1998) *Angew. Chem. Int. Ed*., **37**, 46–62.

Rao, C. N. R., Natarajan, S., Choudhury, A., Neeraj, S., and Ayi, A. A. (2001) *Acc. Chem. Res.*, **34**, 80–7.

Rao, L., Srinivasan, T. G., Garnov, A. Y., Zanonato, P. L., Di Bernardo, P., and Bismondo, A. (2004) *Geochim. Cosmochim. Acta*, **68**, 4821–30.

Roberts, K. E., Wolery, T. J., Atkins-Duffin, C. E., Prussin, T. G., Allen, P. G., Bucher, J. J., Shuh, D. K., Finch, R. J., and Prussin, S. G. (2003) *Radiochim. Acta*, **91**, 87–92.

Runde, W., Bean, A. C., Albrecht-Schmitt, T. E., and Scott, B. L. (2003) *Chem. Commun.*, 478–9.

Runde, W., Bean, A. C., Brodnax, L. F., and Scott, B. L. (2006) *Inorg. Chem.*, **45**, 2479–82.

Staritsky, E. and Cromer, D. T. (1956) *Anal. Chem.* **28**, 913.

Sullens, T. A., Almond, P. M., and Albrecht-Schmitt, T. E. (2006a) *Mater. Res. Soc.*, **893**, 283–94.

Sullens, T. A., Almond, P. M., Byrd, J. A., Beitz, J. V., and Albrecht-Schmitt, T. E. (2006b) *J. Solid State Chem.*, **179**, 1181–90.

Sullens, T. A., Jensen, R. A., Shvareva, T. Y., Albrecht-Schmitt, T. E. (2004) *J. Amer. Chem. Soc.*, **126**, 2676-2677.

Sullivan, J. C., Zielen, A. J., and Hindman, J. C. (1961) *J. Am. Chem. Soc.*, **83**, 3373.

Sykora, R. E., Assefa, Z., Haire, R. G., and Albrecht-Schmitt, T. E. (2004) *J. Solid State Chem.*, **177**, 4413–19.

Sykora, R. E., Assefa, Z., Albrecht-Schmitt, T. E., and Haire, R. G. (2006) *Inorg. Chem.*, **45**, 475–7.

Tabachenko, V. V., Kovba, L. M., and Serezhkin, V. N. (1984). *Koord. Khim.*, **10**, 558–62.

Taulelle, F., Pruski, M., Amoureux, J. P., Lang, D., Bailly, A., Huguenard, C., Haouas, M., Gerardin, C., Loiseau, T., and Ferey, G. (1999) *J Am. Chem. Soc.*, **121**, 12148–53.

Walton, R. I., Millange, F., O'Hare, D. Le Bail, A., Loiseau, T., Serre, C., and Férey, G. (2000) *Chem. Commun.*, **3**, 203–04.

Walton, R. I., Norquist, A. J., Neeraj, S., Natarajan, S., Rao, C. N. R., and O'Hare D. (2001) *Chem. Commun.*, **19**, 1990–91.

Wang, K., Yu, J., Song, Y., and Xu R. (2003) *Dalton Trans.*, 99–103.